University of Ulm

Department of Applied Physiology

Prof. Dr. med. Dr. hc. Frank Lehmann-Horn

Alternative splicing of calcium channel $Ca_V1.1$

Dissertation
Applying for the degree of
Doctor of human biology (Dr. biol. hum.)
Faculty of Medicine, University of Ulm

Submitted by
Natalia Anna Molenda
from Koszalin, Poland
Ulm, 2007

Amtierender Dekan: Prof. Dr. Klaus-Michael Debatin

1. Berichterstatter: PD Dr. Karin Jurkat-Rott

2. Berichterstatter: Prof. Dr. Jürgen Steinacker

Tag der Promotion: 20.07.2007

Contents

LIST OF ABBREVIATIONS
I. INTRODUCTION 1
I.1. Calcium channel 1
I.1.1. Calcium channel family 1
I.1.2. Calcium channel structure and function 2
I.1.3. $Ca_V1.1$ calcium function 5
I.2. Pre-mRNA splicing 7
I.2.1. Signification of splicing 7
I.2.2. Basic splicing reaction 7
I.2.3. Alternative splicing 8
1.3. Alternative splicing of calcium channels 10
I.4. Aims: 15
II. MATERIALS AND METHODS 16
II.1. Molecular biology methods 16
II.1.1. Muscle biopsys 16
II.1.2. Cell culture 16
II.1.3. RNA extraction 17
II.1.4. RT-PCR reaction 18
II.1.5. Strategy of genetic research 19
II.1.6. Separation of DNA fragments by electrophoresis 20
II.1.7. PCR product purification 20
II.1.8. Estimation of band intensity 21
II.2. Plasmids 22
II.2.1. Plasmid pEGFP- CACNA1Sh 22
II.2.1.1. Mutagenesis of pEGFP- CACNA1Sh 22
II.1.2. Plasmid GFP- CACNA1Sr 24
II.2.2.1. Mutagenesis of plasmid GFP- CACNA1Sr 24
II.2.3. Digestion 26
II.2.4. DNA ligation 26
II.2.5. Bacterial Transformation 27
II.2.6. Plasmid isolation and purification 28
II.3. Cell culture and transfection 30
II.3.1 TsA201 30
II.3.2. GLT 30
II.3.3. Transient transfection 32
II.4. Immunofluorescence analysis 32
II.5. Patch clamp analysis and calcium release measurements 33
III. RESULTS 35
III.1. Results of molecular biology investigation 35
III.1.1. Strategy of genetic research 35
III.1.2. Splicing variants in CACNA1S gene 38
III.2. Gene expression 44
III.2.1. Expression of pEGFP-CACNA1Sh in TsA201 cells 44
III.2.2. Expression of plasmid pEGFP- CACNA1Sh in GLT cells 44
IV. DISCUSSION 52
IV.1. Splicing variants in C-terminus of $Ca_V1.1$ 52
IV.2. Splicing variants in first domain 55
IV.3. Premature truncations after third domain. 56

IV.4. Splicing variant in third domain 56
IV.5. Splicing variant in IVS3-S4 region 57
V. SUMMARY 60
VI. REFERENCES 61
VII. ACKNOWLEDGEMENTS 69
VIII: CURRICULUM VITAE 70

List of abbreviations

aa	amino acid
AS	alternative splicing
BTZ	benzothiazepines
CACNA1	calcium channel gene
CACNA1A	P/Q-type calcium channel gene
CACNA1B	N-type calcium channel gene
CACNA1C	cardiac muscle calcium channel gene
CACNA1S	skeletal muscle calcium channel gene
CACNA2D	$\alpha_2\delta$ subunit of calcium channel gene
CACNB	β subunit calcium channel gene
cAMP	Cyclic adenosine monophosphate
$Ca_V1.1$	L-type skeletal muscle calcium channel α_1 subunit
$Ca_V1.2$	L-type cardiac calcium channel α_1 subunit
$Ca_V2.1$	P/Q-type calcium channel α_1 subunit
$Ca_V2.2$	N-type calcium channel α_1 subunit
$Ca_V2.3$	R-type calcium channel α_1 subunit
$Ca_V3.1$	T-type calcium channel α_1 subunit
CDI	calcium-dependent inactivation
cDNA	complementary DNA
C-term	Carboxyl terminus
DCID	distal C-terminal interaction domain
DEPC	diethyl pyrocarbonate water
dH_2O	distilled water
DHP	dihydropyridines
DMEM	dulbeco's modified eagle medium
DMSO	dimethyl sulfoxide
DNA	deoxyribonucleic acid
dNTP	deoxyribonucleotidtriphosphate
ECC	excitation-contraction coupling
ER	endoplasmic reticulum
ESE	exon splicing enhancer
ESS	exon splicing silencer
EST	expressed sequence tag
FCS	fetal calf serum
GFP	green fluorescent protein
GLT	myotubes of the homozygous dysgenic (mdg/mdg) cell line
GLT	homozygous dysgenic (mdg/mdg) cell line obtained from knock-out mousse
G_{max}	maximum conductance
HM	human muscle
HS	horse serum

HT	human myotubes
HVA	high-voltage-activated calcium channels
ISE	intron splicing enhancers
ISS	intron splicing silencer
I-V	current-voltage relationship
kb	kilobase
kDa	kilodalton
LVA	low-voltage-activated calcium channels
MH	maligna hypothermia
mRNA	messenger ribonucleic acid
NMD	nonsense-mediated decay
PAA	phenylalkylamines
PBS	phosphate-buffered saline
PCID	proximal C-terminal interaction domain
PCR	polymerase chain reaction
PEST	proteolytic signal to target proteins for degradation
RNA	ribonucleic acid
RT-PCR	reverse transcriptase PCR
snRNP	small nuclear Ribonucleoprotein Particle
SR	sarcoplasmic reticulum
TsA201	human embryonic kidney cell line expressing simian virus 40 (SV40) T-antigen
UPR	unfolded protein response
$V_{1/2}$	potential for half maximal conductance
WT	wild type

I. INTRODUCTION

I.1. Calcium channel

I.1.1. Calcium channel family

The calcium channels can be divided into subtypes according to their electrophysiological characteristics, and each subtype is encoded by its own gene. Electrophysiological characteristics were first used to classify Ca^{2+} channels by the kinetics of opening and closing, and the conductance and lifetime of individual channels (Bean 1989, Hess 1990). They were initially divided based on their activation threshold, into two subgroups: high-voltage-activated (HVA) (Ca_V1 and Ca_V2) and low-voltage-activated (LVA) Ca^{2+} channels (Ca_V3). Molecular cloning has revealed the existence in humans of at least seven different genes encoding HVA Ca^{2+} channel α_1 subunits and three LVA Ca^{2+} channel genes. Based on the phylogeny underlying these pharmacological and biophysical differences, Ertel et al. (2000) have suggested a more uniform nomenclature for the α_1 subunits of calcium channels which is now commonly used (Fig. 1). Calcium channels were named using the chemical symbol of the principal permeating ion (Ca) with the principal physiological regulator (voltage) indicated as a subscript (Ca_V). The numerical identifier corresponds to the Ca_V channel α_1 subunit gene subfamily 1 to 3.

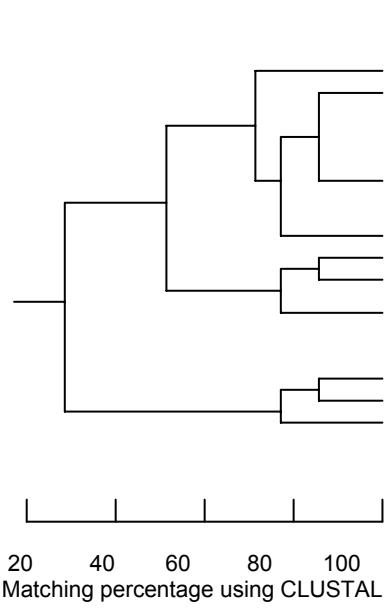

Protein	Gene	Chromosome	Primary tissues
$Ca_V1.1$ (α_{1S})	*CACNA1S*	1q32	skeletal muscle
$Ca_V1.2$ (α_{1C})	*CACNA1C*	12p13.3	heart smooth muscle brain, heart, pituitary, adrenal
$Ca_V1.3$ (α_{1D})	*CACNA1D*	3p14.3	brain, pancreas, kidney, ovary, cochlea
$Ca_V1.4$ (α_{1F})	*CACNA1F*	Xp11.23	retina
$Ca_V2.1$ (α_{1A})	*CACNA1A*	19p13	brain, cochlea, pituitary
$Ca_V2.2$ (α_{1B})	*CACNA1B*	9q34	brain, nervous system
$Ca_V2.3$ (α_{1E})	*CACNA1E*	1q25-31	brain, cochlea, retina, heart, pituitary brain, cochlea, retina
$Ca_V3.1$ (α_{1G})	*CACNA1G*	17q22	brain, nervous system
$Ca_V3.2$ (α_{1H})	*CACNA1H*	16p13.3	brain, heart, kidney, liver
$Ca_V3.3$ (α_{1I})	*CACNA1I*	22q12.3-13-2	brain

Fig. 1. Calcium channels α_1 subunits gene tree and nomenclature [Adapted from (Ertel et al. 2000)].

The complete amino acid sequences of these α_1 subunits are more than 70% identical within a subfamily but less than 40% identical among the three subfamilies. The division of calcium channels into these three families is phylogenetically ancient, as representatives of each are found in the *Caenorhabditis elegans* genome. Consequently, the genes for the different α_1 subunits have become widely dispersed in the genome, and even the most closely related members of the family are not clustered on single chromosomes in mammals (Catterall et al. 2005).

I.1.2. Calcium channel structure and function

Voltage-gated calcium channels mediate calcium influx in response to membrane depolarization and regulate intracellular processes such as contraction, secretion, neurotransmission, and gene expression in many different cell types (Catterall et al. 2006). Their activity is essential to couple electrical signals in the cell surface to physiological events in cells i.e. electrical excitability, synaptic transmission, and excitation-contraction coupling (Catterall et al. 2005).

The calcium channels are complex proteins composed of four or five distinct subunits that are encoded by multiple genes (Fig. 2; Catterall 2000). The α_1 subunit of 190 to 250 kDa is the largest subunit, and it constitutes the conduction pore, the voltage sensor and gating apparatus, and most of the known sites of channel regulation by second messengers, drugs, and toxins (Yamakage et al. 2002).

In order to form a functional calcium channel complex, the α_1 subunit coassembles with at least three accessory subunits: an intracellular β subunit encoded by a CACNB gene, and an extracellular α_2 subunit linked by a di-sulphide bond to the membrane-anchoring δ subunit both of which are encoded by a CACNA2D gene. In skeletal muscle, an additional accessory transmembranal γ subunit is part of the channel complex, related subunits are expressed in heart and brain (Jurkat-Rott and Lehmann-Horn, 2004). The auxiliary subunits have been implicated in function of membrane targeting and modulation of channel properties. Their significance was clarified by heterologous expression in Xenopus oocytes (Cens et al. 1998) and in mammalian expression systems (Takahashi et al. 2003, Neuhuber et al. 1998 Obermair et al. 2005). Moreover, null-mutant mice have provided important information about the roles of Ca^{2+} channel subunits in native tissues.

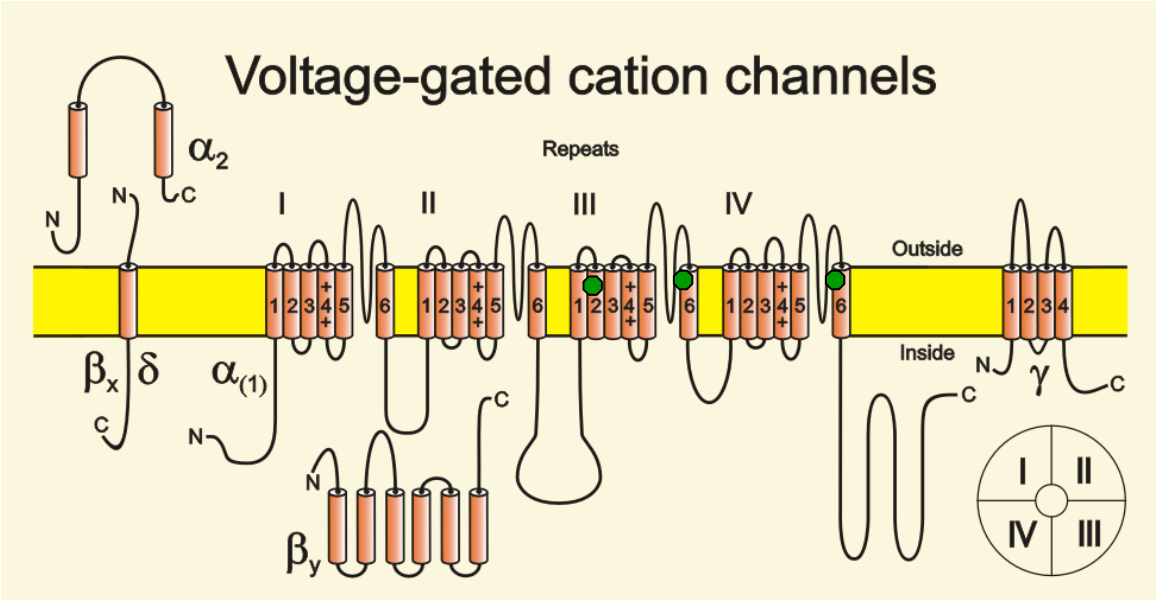

Fig. 2. Schematic representation of voltage-gated cation channels. The α_1 subunit contains as a basic motif a tetrameric association of four domains (I-IV) each containing a series of six transmembrane α -helical segments, numbered S1–S6, which are connected by both intracellular and extracellular loops. The S4 segment serves as the voltage sensor. The pore loop between transmembrane segments S5 and S6 in each domain determines ion conductance and selectivity. Auxiliary subunits ($\alpha_2\delta$, β, and γ) surround the pore-forming α_1 subunit. The helical structures are represented by rods. Connecting loops are drawn as solid lines. Both a short amino-terminal segment and a long carboxy-terminal segment of the α_1 subunit are positioned intracellularly. The single transmembrane segment of S4 in each motif is distinguished by a collection of repeating positively-charged amino acids (arginine or lysine), which are located in every third or fourth position. It is these four positively charged transmembrane segments that are believed to comprise the voltage sensor of Ca_V (McCleskey et al. 1993). The main binding sites for dihydropiridines are marked with green circles.

A mutant of the skeletal muscle α_1 subunit, the muscular dysgenesis mouse, lacks EC coupling and $Ca_V1.1$ currents and dies at birth from respiratory failure (Powell et al. 1996). A knock-out mouse of the skeletal β_{1a} calcium channel subunit results in a very similar lethal muscle phenotype (Gregg et al. 1996). Schredelseker et al (2005) distinguished three distinct effects of the β_{1a} null mutant in skeletal muscle: an ~50% reduction of DHPR membrane expression, severely reduced gaiting charge movement and the complete loss of tetrad formation. The present findings explain that β_{1a} is absolutely required for physical DHPR-RyR interaction.

Homozygous $\alpha_2\delta$-1 knock-out mice die during early embryonic development, therefore, the role of the $\alpha_2\delta$-1 subunit in skeletal muscle were studied using siRNA knock-down (Obermair et al. 2005). This loss-of-function analysis of $\alpha_2\delta$-1 in a differentiated cell type indicated that $\alpha_2\delta$-1 is not required for the targeting of the channel and EC coupling. However $\alpha_2\delta$-1 is a critical determinant of the characteristic slow kinetics of skeletal

muscle L-type calcium currents. Coexpression of $\alpha_2\delta$ subunits with various α_1 subunits in heterologous expression systems demonstrated that $\alpha_2\delta$ enhances the membrane expression of functional Ca^{2+} channels, increases ligand-binding sites, and alters the voltage dependence and kinetics of the calcium currents (Arikkath and Campbell 2003, Mori et al. 1996). In contrast, γ subunit knock-out mice are viable and show only mild effects on current properties (Freise et al. 2000). In adult muscle fibres, by affecting steady state inactivation, the γ_1 subunit can control the availability of $Ca_V1.1$ for voltage-dependent activation of Ca^{2+} release and may change the force responsiveness of the individual fibres. In addition, γ_1 favours the recovery of the resting potential after a long depolarization (reviewed by Melzer et al. 2006).

In summary auxiliary subunits modulate the expression, targeting, gating, and activity of the main α_1 subunit, which, for its part, was in charge of triggering or modulating important physiological processes such as gene expression, excitation-secretion coupling, and excitation-contraction coupling (Rousset et al. 2005).

I.1.3. $Ca_V1.1$ calcium function

$Ca_V1.1$ has dual function: conduct calcium currents and induce excitation-contraction (EC) coupling. $Ca_V1.1$ current require a strong depolarization for activation (high voltage activated), activation kinetics of $Ca_V1.1$ is relatively slow and currents are long lasting (Catterall 2000). Channels are blocked by the organic $Ca_V1.1$ antagonists, including dihydropyridines (DHP, e.g. nifedipine), phenylalkylamines (PAA e.g. varapamil), and benzothiazepines (BTZ e.g. diltiazem) (Mori et al. 1996). The main binding site for calcium antagonists on α-subunit are located in segment IIIS6 and IVS6 as well as the beginning of the C-terminus (Hockermann et al. 1997).

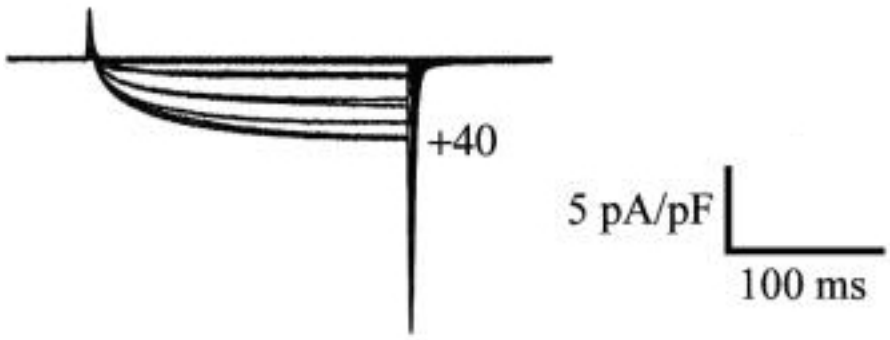

Fig. 3. $Ca_V1.1$ calcium current. The holding potential was -80 mV and 200 ms test pulses to potentials between -50 and +80 mV were applied in 10 mV increments [Adapted from (Flucher et al. 2002)].

Ca_V1 are the main calcium currents recorded in muscle and endocrine cells, where they initiate contraction and secretion (Ertel et al. 2000). Physiological role of this slow calcium inward current is still unclear (Melzer et al. 1995). In skeletal muscle $Ca_V1.1$ channels are crucial for excitation contraction coupling which however does not require influx of Ca^{2+} through these channels. Contraction of these muscle cells is induced by neuronal excitation and further propagation of an action potential along the surface membrane. Inside multiple invaginations of the surface membrane (the T-tubules) the plasmalemma is closely juxtaposed to the membranes of the sarcoplasmic reticulum (SR) in a sandwich-like alignment; a formation called the skeletal muscle triad. The close proximity of the membranes in the triadic junction allows interaction of two distinct Ca^{2+} channels that mediate the transduction from membrane depolarization to the contraction of

the cell, a process called excitation-contraction (EC) coupling (Dulhunty 2006). Upon membrane excitation a voltage-dependant Ca^{2+} channel ($Ca_V1.1$), acts as the voltage sensor and triggers the Ca^{2+} release from intracellular Ca^{2+} stores (sarcoplasmic reticulum; SR) through a sarcoplasmic Ca^{2+} release channel, the ryanodine receptor (RyR). In consequence to RyR opening, Ca^{2+}, released to the cytoplasm, can bind to troponin inside the actin filament to activate the "muscle ratched mechanism" and thus induce muscle contraction.

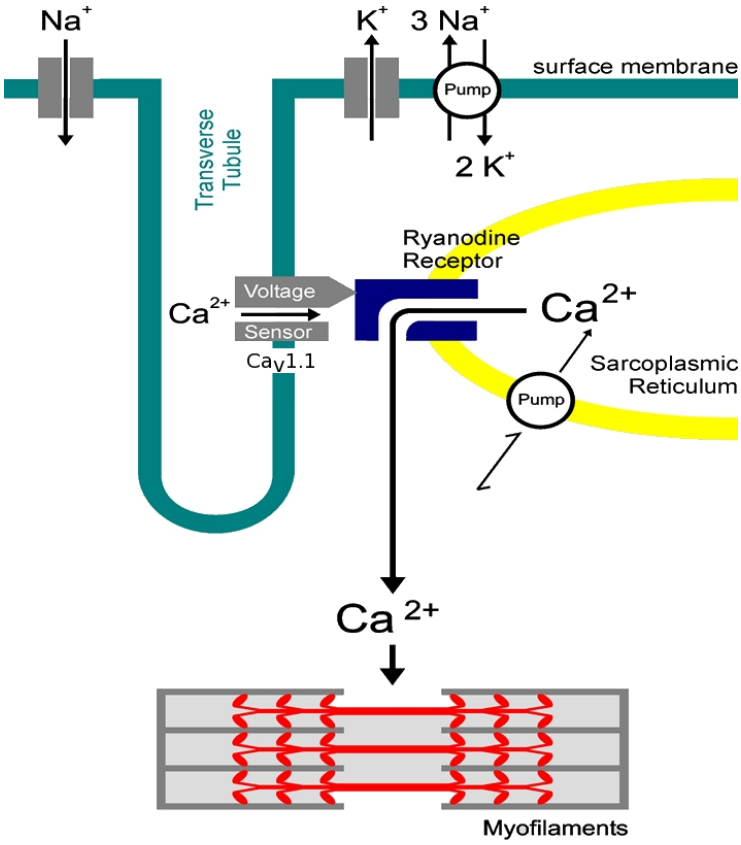

Fig. 4. Excitation-contraction (EC) coupling.

I.2. Pre-mRNA splicing

I.2.1. Signification of splicing

The sequencing of the human genome has demonstrated that humans contain only about 20,000 – 25,000 genes, which is far less then previously expected, vs. ~1,000,000 proteins (International Human Genome Sequencing Consortium, 2004). Therefore, the generation of protein isoforms through regulated alternative splicing is an important step in gene expression of complex organisms.

Analyses of expressed sequence tag (EST) and cDNA datasets estimated that 40 – 60% of human genes are alternative spliced and DNA microarray experiments indicate that 73% of all human genes are alternatively spliced (Matlin et al. 2005), suggesting that alternative splicing of human genes is the rule, not the exception.

I.2.2. Basic splicing reaction

In eukaryotic genes exons, which will make up the mRNA product are interrupted by non-coding introns in DNA and pre-mRNA transcript. The formation of mature mRNAs from primary transcripts (Fig. 3) requires excision of intervening intron sequences and the subsequent joining (splicing) of exons (Matlin et al. 2005). Introns within pre-mRNAs are bounded by conserved sequences that define their ends (splice site consensus sequence).

The splicing reaction is catalyzed by a large and highly dynamic ribonucleoprotein complex, the spliceosome. In size and complexity, spliceosomes are comparable to ribosomes. The spliceosome consists of the five small nuclear Ribonucleoprotein Particles (snRNPs) U1, U2, U4, U5, U6 and ~300 distinct proteins (Nilsen, 2003). In process of pre-mRNA splicing, spliceosome precisely recognizes the exon-intron junction. Four splice signals are essential for accurate splicing: the 5' and 3' splice sites, the polypirimidine tract and the branch site sequence (Goren et al. 2006, Fig. 5).

Splicing proceeds through two sequential transesterification reactions (Fig. 5). The first reaction generates a 2', 5'-phosphodiester bond at the branch point upstream of the 3' splice site and a free 3'-hydroxyl group on the upstream exon. In the second reaction, the newly formed 3'-OH group attacks the phosphodiester bond at the 3' splice site. In consequence, the lariat intron with a 3'-hydroxyl group is released and two exons are

joined together. Following completion of the second step, the spliceosome is disassembled and its components are recycled for further rounds of splicing.

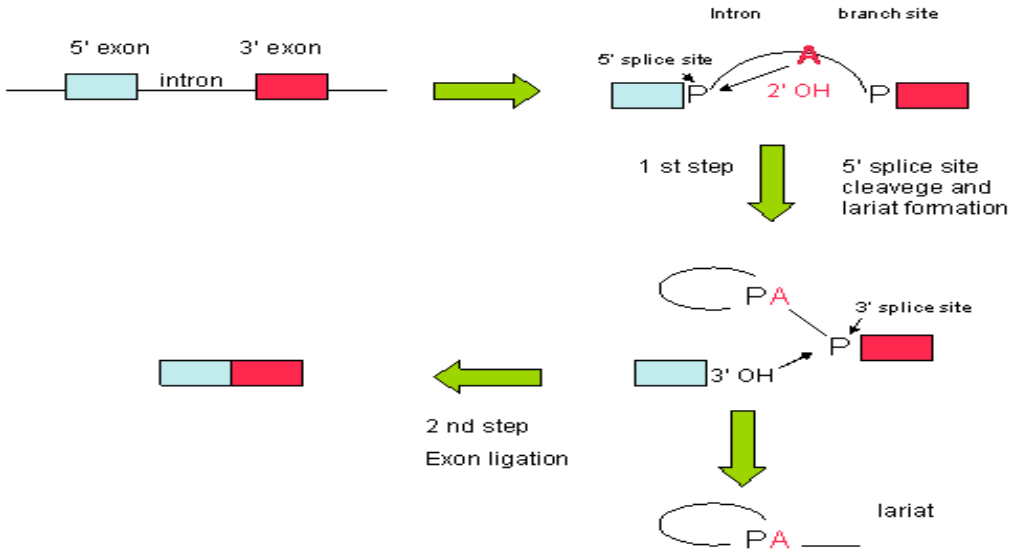

Fig. 5. Chemical mechanism of intron excision by the spliceom. The processing of a pre-mRNA containing two exons and one intron into the ligated exon product and lariat intron is shown.

In addition to the splice-site consensus sequences, a number of auxiliary elements can influence alternative splicing. These are categorized by their location and activity as exon splicing enhancers and silencers (ESEs and ESSs) and intron splicing enhancers and silencers (ISEs and ISSs). Enhancers can activate adjacent splice sites or antagonize silencers, whereas silencers can repress splice sites or enhancers. Exon inclusion or skipping is determined by the balance of these competing influences, which in turn might be determined by relative concentrations of the cognate RNA binding activator and repressor proteins (Matlin et al. 2005).

I.2.3. Alternative splicing

Most alternative splicing events can be classified into five basic splicing patterns: cassette alternative exons, alternative 5' splice sites, alternative 3' splice sites, mutually retained introns and exclusive cassette exons. In addition to the AS mechanisms mentioned above, the exon composition of transcripts is often altered by differential selection of transcription initiation and 3′ end processing/termination sites (Fig. 6), and these events can impact on adjacent or distal AS events in the same transcript (Blencowe 2006). Most alternative splicing events affect the coding sequence, with half of these altering the reading frame and a third apparently leading to Nonsense-Mediated Decay (NMD) of the

RNA product (Matlin et al. 2005). NMD lead to degradation of such mRNA (Stoilov et al. 2002).

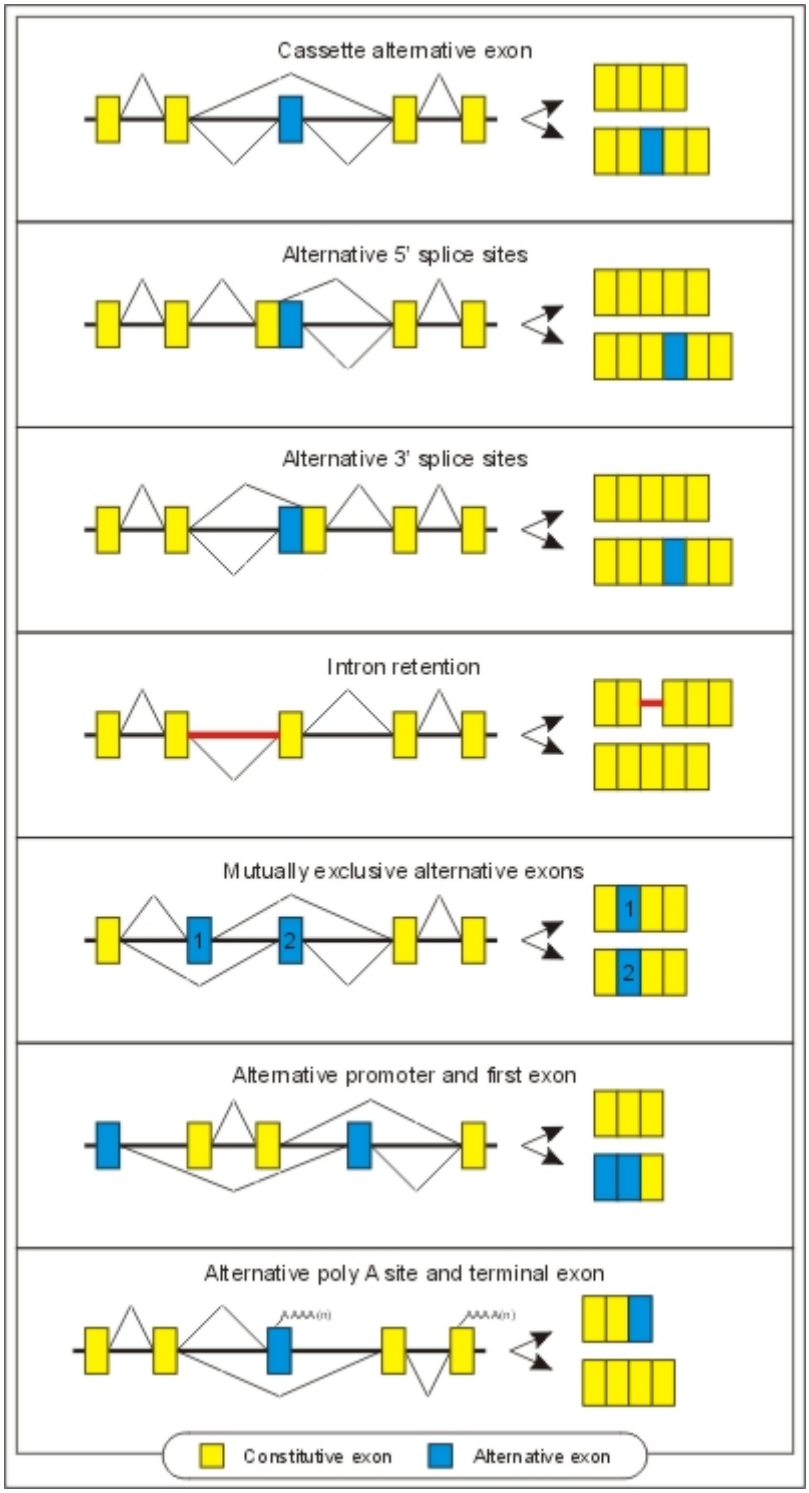

Fig. 6. Alternative spliced events in metazoan transcripts
Types of AS that are responsible for the generation of functionally distinct transcripts are depicted. Blue boxes indicate alternative exons. [Adapted from (Blencowe 2006)]

1.3. Alternative splicing of calcium channels

All aspects of ion channel functions can be altered by alternative splicing, including channel inactivation, -state kinetics, voltage dependency, desensitization time and ligand binding, the effects can range from complete loss of function to subtle effects (reviewed by Stamm et al. 2005). Regulation through alternative splicing can be indirect, involving channel interacting proteins with isoform-specific modulation activities (Helton and Horne 2002). Alternative splicing of channel isoforms is often subject to developmental control, leading, e.g., to developmental specific calcium influxes (Okagaki et al. 2001). Alternative splicing of calcium channels is known to play important role in determining their channels' biophysical properties, their pharmacology, and their ability to be regulated by other proteins (Murbartian et al. 2002, Tang et al. 2007). The observed changes caused by alternative splicing are cell type specific in several cases, which reflects the cell-type specificity of the alternative exon (Chemin et al. 2001, Black 2003, Shen et al. 2006).

Completion of human genome sequence facilitated study of alternative splicing by allowing the identification of intron – exon boundaries. Voltage-gated calcium channels are thought to have evolved by multiple gene duplication from a common ancestral channel gene encoding a one-domain potassium channel (Marban et al. 1998). The intron – exon boundaries or gene structures are therefore not only conserved from one *CACNA1* gene to another, but also from one species to another, for example *Drosophila versus* man (Lin et al. 2004). The gene structure within the *CACNA1* gene family is generally well conserved at coding regions for segments S1–S5 of all four domains (Fig. 7*A*). The remaining regions, especially those coding for the domain interlinkers and the S6 segments of all four domains, show less conserved gene structure suggesting that the encoded protein areas are important for generating functional diversity. These less conserved coding regions coincide with the regions in which alternative splicing produces several different transcripts derived from a single gene (Jurkat-Rott and Lehmann-Horn 2004, Fig. 7*B*). These transcripts generate proteins with similar function and sequence but different expression patterns, the so-called splice isoforms.

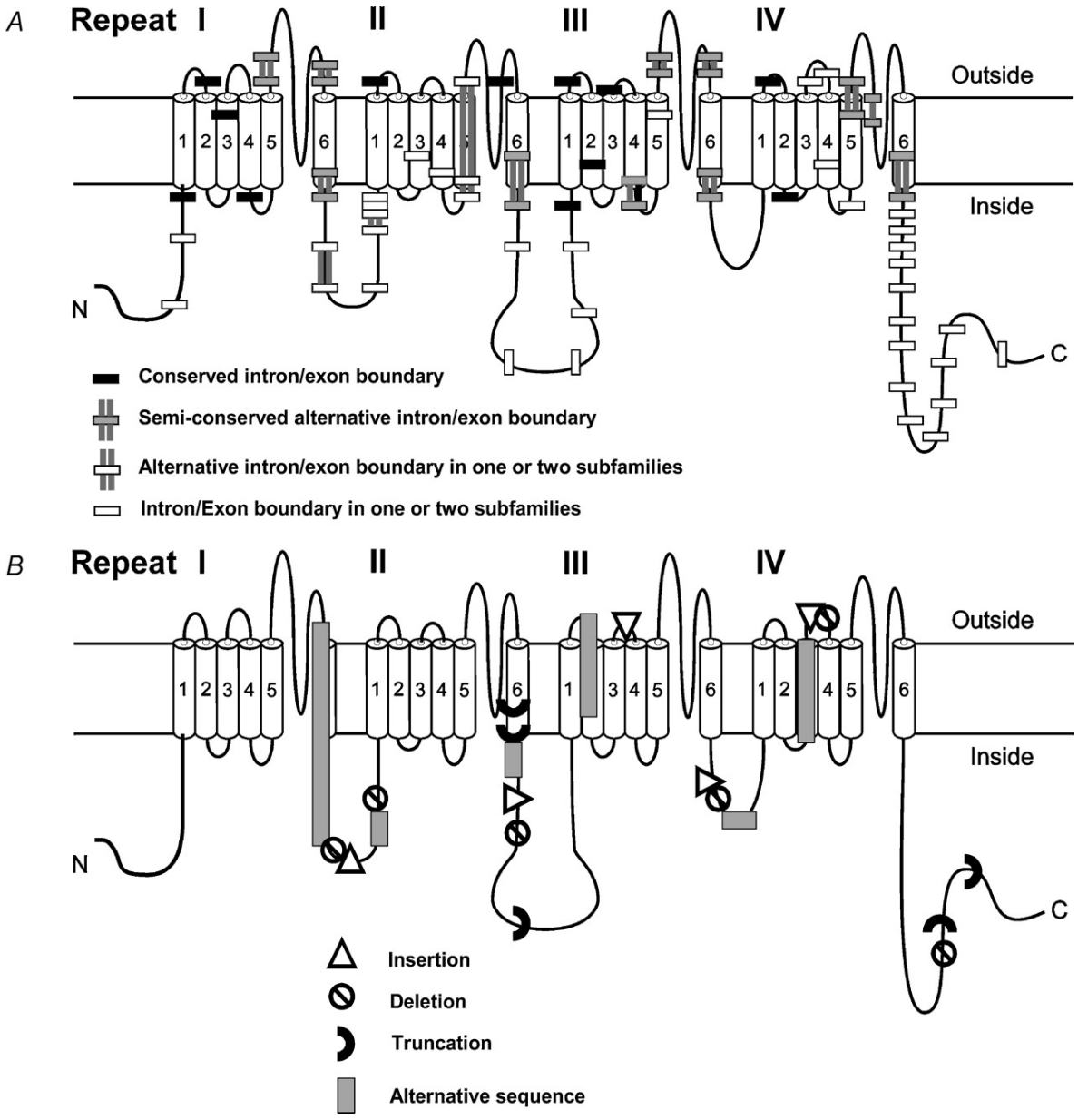

Fig. 7. Scheme of the voltage-gated calcium channel α_1 subunit.
A, conservation of the gene structure at the protein level as determined by protein alignments encoded by all exons of all 10 members of the *CACNA1* family. Each protein region encoded by an exon is delineated by bars. White, black and grey bars indicate degree of conservation as noted in the figure. The following human reference sequences were used at NCBI: $Ca_V2.1$: NP_075461; $Ca_V2.2$: NP_000709; $Ca_V1.2$: NP_000710; $Ca_V1.3$: NP_000711; $Ca_V2.3$: NP_000712; $Ca_V1.4$: NP_005174; $Ca_V3.1$: NP_061496; $Ca_V3.2$: NP_066921; $Ca_V3.3$: NP_066919; and $Ca_V1.1$: NP_000060.
B, regions of the protein that are affected by alternative splicing. Note that the changes now reflect the protein level only (i.e. deletions leading to frame shifts and early truncations are marked as truncation only). The diversity of the primary protein sequence due to insertions, deletions, truncations and alternative sequences is marked by the various symbols. [Adapted from (Jurkat-Rott and Lehmann-Horn 2004)].

The generation of calcium channels splice variants may provide potent means to enrich functional diversity. Tang et al (2004) developed transcript scanning method to probe the human *CACNA1C* gene. The degree of variation turns out to be surprisingly large; 19 of 55 exons comprising this gene were subject of alternative splicing. Overall, the theoretical number of *CACNA1C* splice variants produced by random spliced decisions at each locus would be staggering – 2^{19} combinations. The actual number of splice variations is possible much lower because splicing event is possible not random but linked (Neves et al. 2004). Splice variations of human, cardiac α_1 subunit confer on the channel isoforms altered properties such as sensitivity to blockade by antagonists (Lacinova et al. 2000), regulation by protein kinase (Blumenstein et al. 2002), current density, and activation and inactivation characteristic (Soldatov et al. 1997).

Sites of regulated alternative splicing occur in key functional domains of proteins. The IVS3-IVS4 domain of α_1 subunit family is a conserved site of alternative splicing. Evolutionary conservation, modification of channel function, and tissue-specific expression combine to suggest that alternative splicing in the IVS3-IVS4 region of Ca_V is physiologically important (reviewed by Lin et al. 2004). Alternative splicing of mutually exclusive exons encoding the S3 segment of domain IV of $Ca_V1.2$ channels serves as developmentally regulated switch in cardiac tissue coinciding with major changes in excitation (Diebold et al. 1992). Sperelakis and Shigenobu (1972) first showed that slow channel activity predominated in embryonic chicken harts and gradually becomes less dominant with age. Comparisons of fetal and adult hart and brain uncovered a large IVS3-S4 variability of $Ca_V1.2$. Their electrophysiological characterization revealed shifts in the voltage dependence of activation. The addition of just two amino acids (NP or ET) in the same linker region in the $Ca_V2.1$ and $Ca_V2.2$ channels showed altered biophysical and pharmacological properties (Bourinet et al. 1999, Lin et al. 1997). In $Ca_V2.2$, inclusion of exon 31a in the IVS3-IVS4 region is restricted to the peripheral nervous system, and its inclusion slows the speed of channel activation (Lin et al. 2004). Probably IVS3-S4 linker length correlate with calcium channels current – voltage relationships and voltage – dependent activation characteristics (Tang et al. 2004, Perez-Reyes et al.1990).

The C-terminus makes up a third of the channel protein and is not very well conserved within the *CACNA1* gene family suggesting it to be a region of functional specialization. It is encoded by 3–14 exons, and the protein contains several regulatory elements such as binding sites for calcium, calmodulin (Erickson et al. 2003) and G-proteins (reviewed by Jurkat-Rott and Lehmann-Horn 2004). Alternative splicing in the C-

terminus of Ca_V channels controls the activity and targeting of voltage-gated calcium channels (Krovetz et al. 2000; Soong et al. 2002). The results of Soldatov et al. (1997) $Ca_V1.2$ study show that amino acids encoded by exons 40–42 are important for the voltage dependence of activation and inactivation of the current through these channels, as well as for the kinetics and calcium dependence of inactivation. The deletion of 187 nt from exon 45* in $Ca_V1.2$ channel produces a truncated C-terminus that removes the serine cAMP-dependent protein kinase A site in exon 48 (S1928) (De Jongh et al. 1996, Yang et al. 2005). Exon 45* has been implicated to be important for oxygen sensing (Fearon et al. 2000).

In $Ca_V1.3$ channels within cochlear hair cells the alternate use of exon 41 acceptor sites generated a splice variant that lost the calmodulin-binding IQ motif of the C-terminus. These channels exhibited a lack of calcium-dependent inactivation (CDI), which was independent of the type of coexpressed β subunits (Shen et al. 2006). Calcium channels in hair cells must maintain a finite level of open probability to support spontaneous activity in associated afferent neurons (Robertson and Paki, 2002): too little and the afferent will fall silent, too much and there will be compression of the synapse's dynamic range. Therefore, it is likely that interacting molecular mechanisms are used to ensure an appropriate level of activity.

In $Ca_V2.1$ exclusion of exon 44 from the C-terminus results in more rapid inactivation kinetics (Krovetz et al.2000).$Ca_V2.1$ has also a splice variant, which contains ten substituted residues in a stretch of thirty amino acids in the carboxyl tail adjacent to domain IVS6. Of the ten substitutions, six are located in a region highly similar to the divalent ion binding domain (EF hand) of calcium-binding proteins (Bourinet et al. 1999). The authors did not detect any functional properties that could be attributed to alternative splicing of the EF hand region, it is unlikely that the specific splicing of this highly conserved structural motif is benign. Some possibilities include the interaction of this putative divalent ion binding site with intracellular cations, or the differential interaction at this site of yet-to-be identified proteins that bind to the calcium channel carboxyl terminus. Soong et al. (2002) found $Ca_V2.1$ without exons 43 and 44, splice variation appeared to have substantial effects on CDI, as well as on the overall amplitude of current, possible by variations in channel number.

Cell-specific inclusion of exon 37a in the C-terminus of $Ca_V2.2$ channels represents a mechanism for long-term control of N-type calcium channel activity. Castiglioni et al. (2006) studies of the exons 37a/37b splice site reveal a multifunctional domain in the C-

terminus of $Ca_V2.2$ that regulates the overall activity of N-type calcium channels in nociceptors. N-type calcium channel splice isoforms expressed in a subset of nociceptors gives significantly larger currents, supports increased expression of functional N-type channels and an increase in channel open time as compared to $Ca_V2.2$ channels that contain e37b.

Kanumilli et al. (2005) screened $Ca_V2.1$ in cerebellum of adult rat. They uncovered new splice variations between exons 28 and 34 (some of which predict a premature stop codon) and a new variation in exon 47 (which predicts a novel extended C-terminus). Alternative roles for different C-termini may be the differential subcellular localization of the variants or differential interaction of the variants with intracellular proteins (Maximov et al 1999).

$Ca_V3.3$ contains two regions of alternative splicing: variable inclusion of exon 9 and an alternative acceptor site within exon 33, which leads to deletion of 13 amino acids. Exon 33 variant differ in activation kinetics with no significant difference in deactivation and inactivation kinetics. An unexpected finding of this study was that the effect of exon 9 splicing was highly dependent on the sequence at exon 33. Addition of exon 9 to channels containing the full exon 33 sequence had modest effects on channel gating, slowing recovery from inactivation and the voltage dependence of inactivation (Murbartian et al. 2004).

Gomez-Ospina et al. (2006) discovered that a truncated C-terminus of $Ca_V1.2$ is a transcription factor that can regulate expression of a variety of genes which are important for the function of neurons and muscle cells. This finding reveals an entirely unsuspected function for a well-characterized calcium channel that plays an essential role in electrical tissues.

Taken together, these results indicate that splicing of C-terminus of Ca_V channels modulate channel activity and may provide a site for binding of auxiliary subunits or post-translation processing.

I.4. Aims:

As discussed above, alternative splicing plays a significant role in development and pathology. A lot of work has been undertaken on alternative splicing of ion channels expressed in brain, neurons and heart, but little is known about the splicing variants in skeletal muscle ion channels. Therefore, *CACNA1S* was chosen as target to investigate alternative splicing in our study. As important as defining which type of channel variant is expressed is the question what if any functional correlate may be established between splice variant and type of current. That is why, we pursued two goals:

1. Identification of splice variants in skeletal muscle and myotubes from cell culture at the mRNA level.
2. Determination of their significance for excitation-contraction coupling

Those results will provide useful information to monitor changes on the usage of the entire suite of alternatively spliced exons to help relate altered $Ca_V1.1$ channel function to skeletal muscle physiology and disease.

II. MATERIALS AND METHODS

II.1. Molecular biology methods

II.1.1. Muscle biopsys

The patients for biopsy are exclusively referred to us by anesthesiologist to clarify maligna hypothermia susceptibility. The patient receives information sheet describing all the tests and sings the consent before the biopsy is taken. The local orthopedic and neurological departments perform the muscle biopsy and the sample is transported to our laboratory. After the MH diagnostic test, the remaining vial tissue is cultivated.

II.1.2. Cell culture

Phosphate buffered saline PBS (Gibco, Karlsruhe)
Trypsin (Gibco, Karlsruhe)
Skeletal Muscle Growth Medium (PromoCell, Germany)

Vertebrate skeletal muscles are formed by large syncytial cells, the myotubes, which are innervated by excitatory nerves via the motor endplate. Myotubes were cultured from undifferentiated muscle cells gained by muscle biopsy. Satellite cells are mononuclear progenitor cells found in mature muscle between the muscle fibres. Satellite cells are able to differentiate and fuse to augment existing muscle fibres and to form new fibres. These cells are involved in the normal growth of muscle, as well as regeneration following injury or disease. In undamaged muscle, the majority of satellite cells neither differentiates nor undergoes cell division. Upon muscle damage, satellite cells become activated. Activated satellite cells initially proliferate as skeletal myoblasts before undergoing myogenic differentiation, becoming post-mitotic, and form new myotubes and fuse with existing muscle fibres. This leads to repairing the injured site.

Bioptic muscle tissue was cut into small pieces and incubated in trypsin. Following 30 minutes shaking at 37°C, undifferentiated muscle satellite cells were separated from muscle tissue by filtration through a nylon filter (0.22 μm). These single undifferentiated muscle satellite cells were cultured in Skeletal Muscle Growth Medium (PromoCell, Germany). Cells were maintained at 37°C with 5% CO_2 in a humidified atmosphere (95%). The medium was changed once every three days. Cells were cultured for three to four weeks until myotubes were formed. Before the extraction of RNA, myotubes were washed with PBS (Phosphate buffered saline) twice.

II.1.3. RNA extraction

Reagents for the extraction of RNA:

- TRIzol Reagent (GIBCO BRL, USA)
- Chloroform (Roth, Germany)
- Isopropyl alcohol (Merck, Germany)
- Diethyl pyrocarbonate (DEPC; Roth, Germany)
- DNase I (GIBCO BRL, USA)
- SUPERase IN (Ambion USA)

Total cellular RNA was extracted from homogenized skeletal muscle tissues and cultured cells using TRIzol R (Gibco BRL, USA) according to the manufacturer's protocol.

1. Homogenization

50-100 mg tissue was homogenized with 2 ml TRIzol for 1 min. The insoluble material was removed from the homogenate by centrifugation at 12,000x *g* for 10 minutes at 2 to 8°C. The cleared homogenate solution was transferred to a fresh tube.

2. Phase separation

0.5 ml chloroform was added to each tube. The tubes were shaken vigorously by hand for 15 sec, incubated at 15 to 30°C for 5 min and then centrifuged at no more than 12,000x *g* for 15 min at 2 to 8°C. The aqueous phase, containing RNA, was transferred into a fresh tube.

3. RNA precipitation

To precipitate the RNA, 1 ml of isopropyl alcohol was added to each tube followed by incubation at 15 to 30°C for 10 min and centrifugation at no more than 12,000x *g* for 10 min at 2 to 8°C.

4. RNA washing

2 ml of 75% ethanol was added to the pellet, then mixed by vortexing and centrifuged at no more than 7,500x *g* for 5 min at 2 to 8°C. The RNA pellet was air dried for 5-10 min and solved in 60 µl DEPC (Diethyl pyrocarbonate) water.

To prevent DNA contamination, DNase I was used to digest DNA for 15 min at room temperature. Inactivation of DNase I was performed by heating for 10 min at 65°C. SUPERase IN (Ambion USA) was added to inhibit RNases and RNA was aliquoted and stored at -80°C.

II.1.4. RT-PCR reaction

One step RT-PCR kit (Qiagen, Germany):

- 5×RT-PCR buffer: Tris/HCl, KCl, $(NH_4)_2SO_4$,
- dNTP Mix, 10 mM each
- enzyme mix: Omniscript Reverse Transcriptase, SensiscriptReverse Transcriptase, HotStarTaq DNA polymerase

RT-PCR amplification was carried out in a final volume of 50 µl, using equal amounts (1-2 µg) of total RNA, and 50 pmol forward and reverse primers (Tab. 1)with a one step RT-PCR kit (Qiagen, Hilden, Germany).

Reaction conditions for RT-PCR:

• 50°C for 30 min (first strand cDNA synthesis)
• 95°C for 15 min.
• 35 cycles of: 94°C for 60s, annealing temperature for 60s, 72°C for 60s.
• 72°C for 10 min.

II.1.5. Strategy of genetic research

II.1.5.1. Primers

18 pairs of primers were designed to cover the entire cDNA sequence of *CACNA1S*. Every region amplified by a primer pair overlapped with the next one (Table 1).

Table 1. Primers designed for RT-PCR.

Exons	Forward primer	Backward primer	Tm °C	Product lenght bp
1-9	CaRT1F3: TTCCTGAGATTCTGCCAAGG	CaRT9R3: CTGTGTCAGAGCCACCTTCA	51	1129
2-8	CaRT42F: ATCATCTTGCTCACCATCTTTGC	CaRT8R3: CCCCGAAGGTCCTCATCTA	51	929
7-10	CaRT21F: TATTTTGTCACCCTCATTTTGCTG	CaRT22R: TGCGGCTGGTTGTGGTGCT	54	437
8-10	CaRT8F: ACCAAGGAGCGGGAGAAG	CaRT10R: AGGCGATAGACAGGGTGTTG	52	340
9-15	CaRT9F3: ATGAAGGTGGCTCTGACACA	CaRT26RN: GGTTTCTGCTCCAGCTTCTTG	51	961
10-14	CaRT23F: CCGACATTGGAGGCAGTGGA	CaRT25R: ATCTTCCTGCGTTTTTTCTCCTC	51	825
13-18	CaRT26F: ACTTCATCATCCTTTTCGTCTGT	CaRT27RN: CATGGAATCAGCCCGGATG	52	563
14-18	CaRT14F2: CCCAGAAGGCCAAGGCTGAG	CaRT18R2: CGATGCGGTGACACAGGACACG	55	369
17-26	CaRT17F4: ACGAGGAAGATGAGCCTGAG	CaRT26R3: TGGGTTTTTGGGAATGTAGC	51	1084
18-25	CaRT18F4: ATGCCACCTGGTTTACCAAC	CaRT25R4: TCATGAAGAAGGCAATGAGG	52	780
24-27	CaRT13F: TCTCAGCCATGATGTCCCTCTT	CaRT1R: GTGGTTCATCTGCTCCGACTG	54	443
25-26	CaRT1F: CATCTTTGTGGGCTTCGTCATT	CaRT13R: TGGTATGGGTTTTTGGGAATGT	54	150
26-35	CaRT2F: CACCTCCTCCTACTTTGAATACCT	CaRT35R3: AGAACTTCCCAAAGCCCAGA	52	971
27-34	CaRT27F3: AGTCGGAGCAGATGAACCAC	CaRT34R3: ATGGCCTTGAACTCATCCAG	51	790
34-40	CaRT34F3: ACTACCTCACCCGGGACTG	CaRT40R3: CGTTGGCATTGTTGGTATTG	51	843
37-42	CaRT37F3: AACCAGCATGAAGCTCTTGG	CaRT42R3. AGCAGTCCCTTCAGCATCTC	52	678
39-44	CaRT39F3: CGGACCATTGAGGAAGAGG	CaRT44R3: CATTGGTCATGCCAGCTCTA	51	990
34-44	CaRT34F3: ACTACCTCACCCGGGACTG	CaRT44R3 CATTGGTCATGCCAGCTCTA	51	1514

II.1.6. Separation of DNA fragments by electrophoresis

TBE buffer (Tris-Borate 45 mM; EDTA 1mM, pH 8.2 - 8.4)
10 x loading buffer (15 % Ficoll, 0.1 % Bromphenol blue)
Ethidium bromide (0,7 mg/ml) Eurobio France

DNA fragments were separated by agarose gel electrophoresis. Usually, 2% (w/v) agarose gel in the basic buffer TBE was used. DNA samples were mixed with 10 x DNA loading buffer in a ratio of 10:1. As a length standard, 10 ng of 1 kb marker (Invitrogen, Karlsruhe, Germany) were used. The gels were stained with ethidium bromide (0, 7 mg/ml), nucleic acids were detected by UV illumination and the result documented photographically.

II.1.7. PCR product purification

DNA and gel band purification kit (Amersham Pharmacia Biotech Inc., USA):

- Capture buffer – buffered solution containing acetate and chaotrope
- GFX columns – MicroSpin^{TM} columns pre-packed with glass fiber matrix
- Wash buffer Tris- EDTA buffer (10 mM Tris-HCl pH 8.0, 1mM EDTA) dissolved in 48 ml absolute ethanol

Following electrophoresis, DNA bands were cut out and purified using the DNA and gel band purification kit (Amersham Biosciences, Freiburg, Germany):

1. Denaturation / solubilization

   For each 10 mg of the gel slice 10 ml of capture buffer was added into an Eppendorf tube. The samples were mixed by vortexing and incubated at 60°C for 15 min.

2. Capture

   After the agarose was completely dissolved, the samples were briefly centrifuged, transferred to the GFX column, incubated at room temperature for 1 min and centrifuged at full speed for 30 sec.

3. Washing / Drying

   The flow-through was discarded and 500 µl of wash buffer was added to each sample followed by a new centrifugation at 12.000 x g for 30 sec.

4. DNA elution

The GFX column was transferred to a collection tube and 45 µl of double distilled water - ddH_2O was applied to each tube. After 2 min incubation the purified DNA was recovered by centrifugation at full speed for 1 min.

The purified samples were sent to MWG Company (Ebersberg, Germany), where they were sequenced using the BIG Dye Termintor Cycle Sequencing Kits (Applied Biosystems, USA) with ABI 377 HT sequencing machine (Applied Biosystems, USA).

II.1.8. Estimation of band intensity

Every gel was photographed in UV light using camera. Scion Image 4.0.3.2 (Scion Corporation, USA) software was used to define size and intensity of RT-PCR bands on ready photos. To calculate the normalized ratio of splicing variant and full-length variant, two formulas were used:

$Rn = In \times An / (In \times An) + (Is \times As)$
$Rs = Is \times As / (Is \times As) + (In \times An)$

Rn - The normalized ratio of full-length variant
Rs - The normalized ratio of splicing variant
In - Band intensity of full-length variant
Is - Band intensity of splicing variant
An - Band area of full-length variant
As- Band area of splicing variant

This method estimated ratio of full-length variant and its splicing variants.

II.2. Plasmids

II.2.1. Plasmid pEGFP- CACNA1Sh

GFP is a cytosolic polypeptide which emits green fluorescent light in the absence of exogenous substrates or cofactors, it was cloned from the jellyfish *Aequorea victoria*, (Prasher 1992). It was introduced into pladmid to identify successful transfected cells. pEGFP-C3 ("enhanced green fluorescent protein", Clontech, Heidelberg) plasmid was used to obtain GFP/CACNA1Sh fusion constructs.

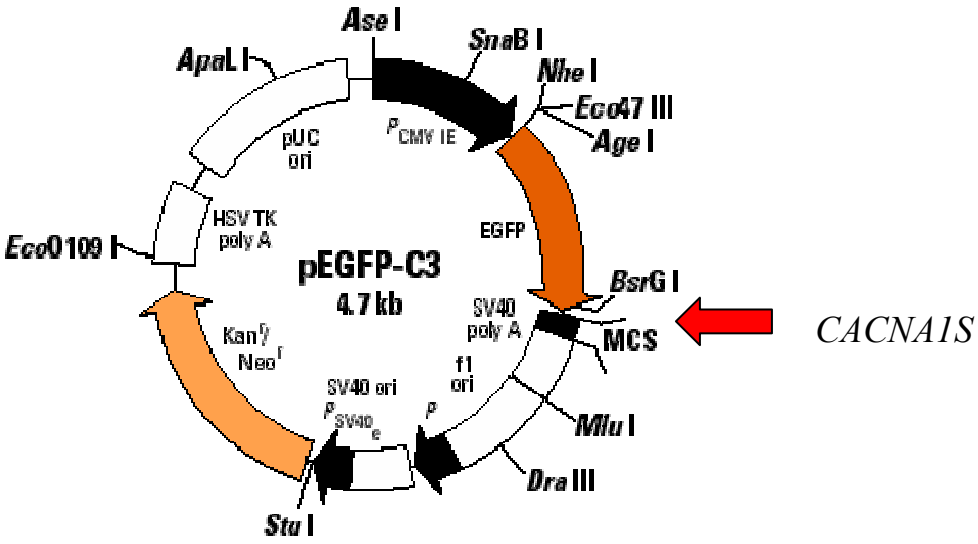

Fig. 8. Schematic representation of the pEGFP-C3 vector. The important enzymatic restriction sites are indicated.

II.2.1.1. Mutagenesis of pEGFP- CACNA1Sh

Pfu polymerase (Fermentas, St. Leon-Rot)

FastDigest (Fermentas, St. Leon-Rot)

Quick ligation kit (New Englands Biolabs, USA)

To obtain an enhanced expression system, human *CACNA1S* cDNA was isolated from pCEP4-CACNA1S vector (gift from Kirk Hogan, USA) using XhoI and XbaI. The fragment was than gel-purified and cloned in frame into pEGFP-C3, in front of the GFP stop codon (Fig. 8).

In order to create a plasmid containing the splicing variant missing exon 29, a restriction site for AscI was inserted into the cDNA sequence by introducing silent point mutations via PCR mutagenesis using Forward primer 5' TATGCCCTGAAGGCGCGCCCACTGA-3' and reverse primer 5' CTGCCCGGCTCAGAAGCTTGATCAG-3'.

Table 2. Mutagenesis of plasmid pEGFP- CACNA1Sh

Variant	Restriction sites	Localization	Primers Exons	Product length
Deletion of exons 39, 40	BstE II G/GTNACC GGTGACC Xba I T/CTAGA	4265-4272 Exon 41	M5F + M5R 34/35 - 41	889- standard 509 - variant
Alternative 5' splice site of exon 40	BstE II G/GTNACC GGTGACC Xba I T/CTAGA	4266-4272 Exon 41		889- standard 811 - variant
Deletion of exon 29	AscI GG/CGCG/CC GGCCCGCC Hind III A/AGCT/T	3281-3289 3732-3738	M4F + M4R 25 - 30	481 - standard 424 - variant

Three splicing variants were inserted into pEGFP-C3, in all cases a pair of restrictions enzymes was chosen to remove a part of the cDNA. In parallel the desired fragments were obtained by RT-PCR reaction from human muscle. Primers were designed to amplify exclusively the chosen splicing variants:

1. skipping of exon 39 and 40
M41R F –5'GTACAGATCCAGTGTCCACTATG-3'
M41 R –5'CATAGTGGACACTGGATCTGTAC-3'

2. alternative 5' site of exon 40
M40 F2 –5' GGAATATTCCGGAGACCCCTCCAG-3'
M40 R2 –5'CTGGAGGGGTCTCCGGAATATTCC-3'

3. skipping of exon 29
To obtain this variant it was not necessary to design special primers. Using human myotubes as a template enough material could be obtained.

II.1.2. Plasmid GFP- CACNA1Sr

In this plasmid the coding sequence of the α_1 subunit of the rabbit skeletal muscle calcium channel (*CACNA1S*) is inserted "in-frame" and downstream of the coding region of a modified GFP, cloned in a mammalian expression vector. GFP is fused to the N terminus of the α_1 subunit to avoid the potential loss of the label by physiological truncation of the carboxyl terminus. This vector was kindly provided by Manfred Grabner (Innsbruck, Austria).

II.2.2.1. Mutagenesis of plasmid GFP- CACNA1Sr

Similar variants as those described in II.2.1.1. were also constructed for GFP-CACNA1Sr which contains the rabbit homolog of *CACNA1S*. Deletions were created by PCR splicing, using pGFP- CACNA1Sr as a template. To delete a desired fragment, a pair of primers flanking the region where the deletion will be made (primers 1 and 4) and additionally 2 complementary primers comprising a region of -25 bp to +25 bp related to the junction point (primers 2 and 3) were designed. The procedure is shown in Fig. 9.

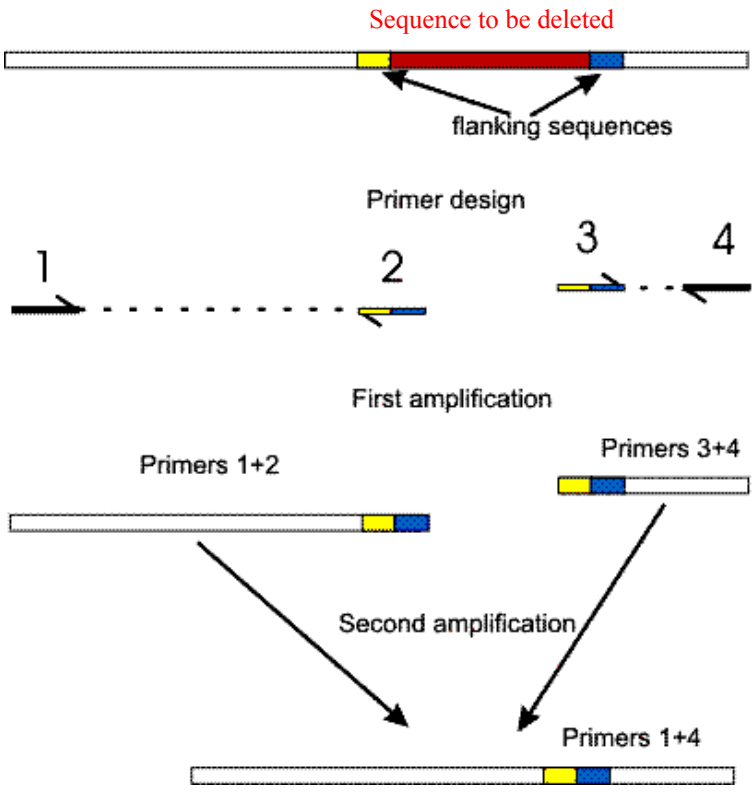

Fig. 9. Scheme of deletion by PCR splicing

Flanking primers:

1,2. alternative 5' site of exon 40 and skipping of exon 39 and 40
BglII-F –5'-gtaactttgagcaggccaacgagg-3'
EcoRV-R –5'-ccatcgattgaattcgagctcgg-3'

3. skipping of exon 29
XhoI-F –5'-gcacaagggctccttctgccgcaac-3'
BglII-R –5'-ggaagtgctcctgaatgaggaatgtggc-3'

For both C-term variants the same pair of flanking primers was used. All primers were situated upstream of restriction sites indicated in their names. These enzymes were used to cut PCR products and vector prior to ligation.

Complementary primers:

1. alternative 5' site of exon 40

Alt.40-F –5'-gcgatggaggagaggatcttccggagaccgctccagtttgctgagatagaaatg-3'
Alt.40-R –5'-catttctatctcagcaaactggagcggtctccggaagatcctctcctccatcgc-3'

2. skipping of exon 39 and 40

Δ39, 40-F –5'-gaaggacaccgtgcagatccagcgtccactgtgaaagggagttcc-3'
Δ39, 40-R –5'-ggaactccctttcacagtggacgctggatctgcacggtgtccttc-3'

3. skipping of exon 29

Δ29-F –5'-atcattgacgtcatcctcagcgagatcgacgacccagacgagagcgcccgcat-3'
Δ29-R –5'-atgcgggcgctctcgtctgggtcgtcgatctcgctgaggatgacgtcaatgat-3'

PCR amplification was carried out in a final volume of 50 µl, using equal amounts (2 µg) of plasmid, and 50 pmol forward and backward primers with Taq polymerase. After first amplification 10 µl from both PCR reactions were combined and used as template for the final amplification with Pfu polymerase (Fermentas, St. Leon-Rot).

The PCR program used for first amplification was:

- • 94°C for 2 min.
- • 30 cycles of: 94°C for 60s, 60°C for 60s, 72°C for 60s.
- • 72°C for 3 min.

The PCR program used for final amplification was:

- • 95°C for 3 min.
- • 30 cycles of: 95°C for 90s, 60°C for 90s, 72°C for 4 min.
- • 72°C for 5 min.

DNA fragments were separated by agarose gel electrophoresis. After electrophoresis, DNA bands were cut out and purified using the DNA and Gel band purification kit (Amersham Biosciences, Freiburg).

II.2.3. Digestion

FastDigest (Fermentas, St. Leon-Rot)

The purified samples of PCR products and plasmid were double digested using the FastDigest system (Fermentas, St. Leon-Rot). Generally, digests were prepared in 20 µl total volumes, with 1 µl of each restriction enzyme and incubated at 37°C for 5 - 15 minutes.

II.2.4. DNA ligation

Quick ligation kit (New Englands Biolabs, USA)

DNA ligation was performed using Quick ligation kit (New Englands Biolabs, USA) in a volume of 20-40 µl. About 50 ng vector was used in one ligation. The ratio of vector to insert was 1:2-3.

II.2.5. Bacterial Transformation

TYGPN medium:

- Trypton 20.0 g
- Yeast Extract 10.0 g
- 9.2 ml Glycerol 87 % 11.3 g
- Na_2HPO_4 5.0 g
- KNO_3 10.0 g
- ddH_2O to 1000 ml

LB medium:

- Bacto – tryptone 10 g
- Bacto – yeast – extract 5 g
- NaCl 10 g
- ddH_2O to 1000 ml

LB plates:

- 200 ml LB medium
- 3 g select agar (1.5 %)
- Antibiotic (50 µg/ml)

The plasmids were amplified by transformation into the bacterial strain DH5α (Invitrogen, Karlsruhe) as follows:

1. Thawing

   50 - 100µl of supercompetent cells were gently thawed from -70°C on ice.

2. Adding DNA

   1 µg of plasmid DNA was added to the cells and incubated on ice for 30 minutes.

3. Heat shock

   The reaction was heat pulsed at 42°C in a water-bath for 1 min and then immediately placed on ice for 5 minutes.

4. Recovery and proliferation

   500 µl of TYGPN (tryptone-yest-glycerine) medium was then added and the cells were incubated at 37°C for 60 minutes.

5. Selection

Finally 200-300 µl of the end volume was plated onto agar plates containing the appropriate antibiotic.

II.2.6. Plasmid isolation and purification

QIAfilter Midi Kit (Qiagen, Hilden, Germany):

- Buffer P1 (resuspension buffer) 50 mM Tris·Cl, pH 8.0; 10 mM EDTA, 100 µg/ml RNase A -
- Buffer P2 (lysis buffer) 200 mM NaOH, 1% SDS (w/v)
- Buffer P3 (neutralization buffer) 3.0 M potassium acetate, pH 5.5
- Buffer FWB2 (QIAfilter wash buffer) 1 M potassium acetate pH 5.0
- Buffer QBT (equilibration buffer) 750 mM NaCl; 50 mM MOPS, pH 7.0; 15% isopropanol (v/v); 0.15% Triton® X-100 (v/v)
- Buffer QC (wash buffer) 1.0 M NaCl; 50 mM MOPS, pH 7.0; 15% isopropanol (v/v)
- Buffer QF (elution buffer) 1.25 M NaCl; 50 mM Tris·Cl, pH 8.5; 15% isopropanol (v/v)
- Buffer QN (elution buffer) 1.6 M NaCl; 50 mM MOPS, pH 7.0; 15% isopropanol (v/v)
- TE 10 mM Tris·Cl, pH 8.0; 1 mM EDTA

Plasmid DNA was isolated from bacteria using the QIAfilter Midi Kit (Qiagen, Hilden). QIAGEN plasmid purification protocols are based on a modified alkaline lysis procedure, followed by binding of plasmid DNA to QIAGEN Anion-Exchange Resin under appropriate low-salt and pH conditions. RNA, proteins, dyes, and low-molecular weight impurities are removed by a medium-salt wash. Plasmid DNA is eluted in a high-salt buffer and then concentrated and desalted by isopropanol precipitation.

II.2.6.1. Midi-Preparation Procedure:

1. Growing cultures

A single colony from a freshly streaked selective plate was picked and added to 3 ml LB medium containing the appropriate selective antibiotic. Culture was incubated for approx. 8 h at 37°C with vigorous shaking (approx. 300 rpm).

Than the starter culture were diluted 1/500 into selective LB medium and grown at 37°C for12–16 h with vigorous shaking (approx. 300 rpm).

2. Bacteria pelleting

The bacterial cells were harvested by centrifugation at 6000 x *g* for 15 min at 4°C.

3. Bacteria resuspending

The bacterial pellet was resuspended in 4 ml Buffer P1.

4. Bacteria lysing

4 ml Buffer P2 was added and mixed thoroughly by vigorously inverting the sealed tube 4–6 times, and incubated at room temperature (15–25°C) for 5 min.

5. Lysate precipitating

4 ml chilled Buffer P3 were added to the lysate, and mixed immediately and thoroughly by vigorously inverting 4–6 times. Than the lysate was incubated 15 min on ice.

6. Centrifugation

Lysate was centrifuged at 12,000 rpm for 30 min at 4°C. Supernatant containing plasmid was removed promptly and inserted into fresh tube. Than supernatant was centrifuged again at 12,000 rpm for 30 min at 4°C.

7. QIAGEN-tip equilibration

A QIAGEN-tip 100 was equilibrated by applying 4 ml Buffer QBT, and allowing the column to empty by gravity flow.

8. Plasmid binding

The supernatant from step 6 was applied to the QIAGEN-tip and entered the resin by gravity flow.

9. Washing

The QIAGEN-tip was washed with 2 x 10 ml Buffer QC.

10. Eluting

DNA was eluted with 5 ml Buffer QF.

11. Isopropanol precipitating

DNA was precipitated by adding 3.5 ml room-temperature isopropanol to the eluted DNA. It was mixed and centrifuged immediately at 11,000 rpm for 45 min at 4°C. Supernatant was carefully decanted.

12. Ethanol precipitating

DNA pellet was washed with 2 ml 70% ethanol at room-temperature, and centrifuged at 11,000 rpm for 30 min. Supernatant was carefully decanted without disturbing the pellet.

13. Plasmid dissolving

The pellet was air-dried for 5–10 min, and the DNA was redissolved in 50 µl dd water.

Plasmid DNA concentration and purity was determined via absorption measurement with 260 and 280 nm in a spectrophotometer (Pharmacia LKB-UltrospecIII).

II.3. Cell culture and transfection

II.3.1 TsA201

Solutions used for cell culture:

- DMEM medium - Dulbecco's modified Eagle's medium (Gibco, Karlsruhe, Germany)
- FCS - Foetal calf serum (Gibco, Karlsruhe, Germany)
- PBS - Phosphate buffered saline without calcium, magnesium, and sodium bicarbonate (PAA Laboratories, Cölbe, Germany)
- Trypsin/EDTA (Gibco, Karlsruhe, Germany)

TsA201 cells are a simian virus 40 (SV40) T- antigen expressing derivative of the human embryonic kidney (HEK-293) cell line and support replication of plasmids containing the SV 40 origin of replication. These cells were chosen for their high transfection efficiency (Margolskee et al. 1993).

TsA201 cells were cultured in MEM supplemented with 10 % FCS. Cells were maintained at 37°C with 5 % CO_2 in a humidified atmosphere (95 %) and split three times per week. For splitting cells, 1 ml of Trypsin/EDTA (0.15 % Trypsin, 0.08 % EDTA in PBS w/o Ca^{2+} and Mg^{2+}) was used to dislodge cells from the base of the culture flask. After 2-3 minutes, the enzyme reaction was stopped with 5 ml of MEM. Cells were then centrifuged at 1000 rpm for four minutes and, following re-suspension, placed in two new culture flasks containing 5 ml of the appropriate medium.

II.3.2. GLT

Solutions used for cell culture:

- DMEM medium - Dulbecco's modified Eagle's medium
- FCS - Foetal calf serum
- HS – horse serum

- PBS - Phosphate buffered saline without calcium, magnesium, and sodium bicarbonate
- Trypsin/EDTA
- Rat tail collagen (Typ 1, C 7661) from Sigma-Aldrich (Taufkirchen, Germany),

GLT myotubes of the homozygous dysgenic (mdg/mdg) cell line obtained from knock-out mousse, which do not have $Ca_V1.1$ channel, but still forms regular junctions containing RyRs. This line was originally generated by transfection of mdg myoblasts with a plasmid-encoding Large-T Antigen (Powell et al. 1996). Transient transfection of myotubes of dysgenic cell line GLT with expression plasmid encoding CACNA1S restores expression of this channel in the triads, $Ca_V1.1$ currents, and skeletal muscle EC coupling (Flucher et al. 2000).

GLT myoblasts were expanded in growth medium (DMEM with 1% glutamine (200 mM), 10% FCS, and 10% HS) at 10% CO_2 and 37°C and passaged before reaching 80% confluency using trypsin detachment. To obtain myotubes, cells were plated onto carbon- and collagen-coated coverslips in 35-mm dishes. After reaching high confluency, growth medium was exchanged for fusion medium (DMEM with 1% glutamine (200 mM) and 2% HS). The onset of myoblast fusion occurred 2 days after changing to differentiation medium and continued for up to 1 week. Eventually all myoblasts fused and formed short (two to six nuclei) to medium-long (20-40 nuclei) myotubes with a low degree of interconnection.

When cells reached higher passages, new cells were thawed from the liquid nitrogen stocks. Cells were thawed slowly at room temperature, resuspended in 5 ml fresh medium, then centrifuged at 1000 rpm for four minutes and, following re-suspension, placed in two new culture flasks containing 5 ml of the appropriate medium. To renew the liquid nitrogen cell stocks, cells were grown to confluence in 100 ml flasks, resuspended in 10 ml medium, centrifuged for 10 minutes at 2000 rpm, resuspended in 8-10 ml special freezing medium containing 20 % DMSO, 20 % FCS, and 60 % medium without antibiotics, and distributed in labeled cryotubes. The cryotubes were placed in cold ethanol 70 %, and kept overnight at -80^oC. The next day, the cryotubes were immersed in liquid nitrogen.

II.3.3. Transient transfection

Fugene 6 (Roche Diagnostics, Mannheim, Germany).

TsA201 transient transfection was performed with the assistance of the Fugene 6 from Roche Diagnostics (Mannheim, Germany). For electrophysiological measurements of currents, transiently transfected TsA201 cells were plated in 35 mm dishes 16h before measurements.

GLT cells were transfected at the onset of fusion (day 4) with Fugene 6, according to the manufacturer's instructions (Roche Diagnostics). A total of 2 μg of plasmid DNA was used per 35-mm culture dish. Measurements were made from the myotubes four days later.

II.4. Immunofluorescence analysis

Differentiated cultures were simultaneously immunostained as described by Flucher et al. (1994) with the monoclonal $Ca_V1.1$ antibody mAb1A at a dilution of 1:2,000, together with a rabbit affinity-purified anti-GFP antibody (Molecular Probes, Eugene, OR) at a dilution of 1:5,000 or the affinity-purified antibody 162 against the RyR1 at a dilution of 1:5,000. An Alexa-488-conjugated goat anti-rabbit antibody (Molecular Probes, Eugene, OR) was used with anti-GFP so that the antibody label and the intrinsic GFP signal were both recorded in the green channel. Alexa-594-conjugated goat anti-mouse (Molecular Probes, Eugene, OR) was used to detect anti-$Ca_V1.1$ Controls, for example the omission of primary antibodies and incubation with inappropriate antibodies, were routinely performed. Images were recorded on a Zeiss Axiophot microscope equipped with a cooled CCD camera and METAVIEW image-processing software (Universal Imaging, West Chester, PA). Analysis of $Ca_V1.1$ expression and clustering was performed by systematically screening of cover glasses for well differentiated transfected (GFP-positive) myotubes (GLT). Based on the RyR1 expression, and GFP-$Ca_V1.1$ expression GLT myotubes were classified as normal (clustered in triads), not targeted (ER/SR distribution) or absent (nontransfected myotubes). All counts were performed in duplicate cover glasses from at least four independent experiments. Data are given as mean +/- S.E. Statistical significance was determined by unpaired Student's *t* test.

II.5. Patch clamp analysis and calcium release measurements

Calcium currents were recorded with the whole cell patch clamp technique at room temperature (20–23°C). Patch pipettes had resistances of 1.5–3 megohms when filled with (mM): 145 cesium aspartate, 2 $MgCl_2$, 10 HEPES, 0.1 Cs-EGTA, 2 Mg-ATP (pH 7.4 with CsOH). Fluorescent signals of intracellular calcium transients were collected microphotometrically (Photon Technology International, S. Brunswick, NJ) during whole cell recordings by including 0.2 mM pentapotassium Fluo-4 (Molecular Probes, Eugene, OR) in the pipette solution. The bath solution contained (mM): 10 $CaCl_2$, 145 tetraethylammoniumchloride, 10 HEPES (pH 7.4 with tetraethylammoniumhydroxide). Currents were recorded with an Axopatch 200A amplifier (Axon Instruments Inc., Foster City, CA, USA). Data acquisition and command potentials were controlled by pClamp software (version 7.0, Axon Instruments). Test pulses were preceded by a 1 s prepulse to -50 mV to inactivate endogenous Ca_V3 channels. Currents were determined with 200 ms depolarizing steps from a holding potential of -80 mV to test potentials between -50 and +80 mV in 10 mV increments. Leak currents were digitally subtracted by a P/3 prepulse protocol. Cell capacitance (Cm) was determined by integration of the capacity transient resulting from a +10 mV pulse applied from the holding potential and was used to normalize ionic (pA/pF) and gating (nC/mF) currents obtained from different myotubes. Recordings were low-pass Bessel filtered at 2 kHz and sampled at 5 kHz. Only currents with a voltage error ≤ 5 mV attributable to series resistance were further analyzed with Clampfit® 8.0 (Axon Instruments Inc., FosterCity, CA) and SigmaPlot® 8.0 (SPSS Science, Chicago, USA) software. For the selection of recordings for the kinetic analysis additional constraints (noise and stability) applied. The activation phase of currents (0 to current level to 98% of peak) was fitted with both a single and a double-exponential function using Clampfit® 8.0 software. In both cases (CACNA1Sr and CACNA1Sr Δ29) the traces were best fit with a double exponential function:

$$I = A_{fast} \cdot \left(\exp\left(-t / \tau_{fast}\right)\right) + A_{slow} \cdot \left(\exp\left(-t / \tau_{slow}\right)\right) + C \qquad (1)$$

where I is the current, A_{fast}, and A_{slow} are the individual steady state current amplitudes, while τ_{fast}, and τ_{slow} are their specific time constants of activation, and C represents the steady state peak current.

The current-voltage dependence was fitted according to:

$$I = G_{\max} \cdot \left(V - V_{rev}\right) / 1\left(1 + \exp\left(-\left(V - V_{1/2}\right) / k\right)\right) \qquad (2)$$

where, G_{max} is the maximum conductance of the Ca^{2+} channels, V_{rev} is the extrapolated reversal potential of the Ca^{2+} current, $V_{1/2}$ is the potential for half maximal conductance and k is the slope factor.

The voltage dependence of the Ca^{2+} conductance was fitted according to a Boltzmann distribution:

$$G = G_{\max} / \left(1 + \exp\left(-\left(V - V_{1/2}\right)/k\right)\right) \qquad (3)$$

Data are given as mean +/- SEM. Statistical significance was determined by unpaired Student's *t* test.

III. RESULTS

III.1. Results of molecular biology investigation

III.1.1. Strategy of genetic research

18 pairs of primers were designed to cover the entire cDNA sequence of *CACNA1S*. Every region amplified by a primer pair overlapped with the next one (Fig. 10). In order to detect all splicing variants, additional two primer pairs were constructed for every loop, domain and for the C-terminus region. On figure 10 we can see this in detail for first domain, two forward primers are placed in exon 1 and 2, respectively and two reverse primers in exon 8 and 9. Even if one of these exons is skipped we will get the PCR product with other primers pair.

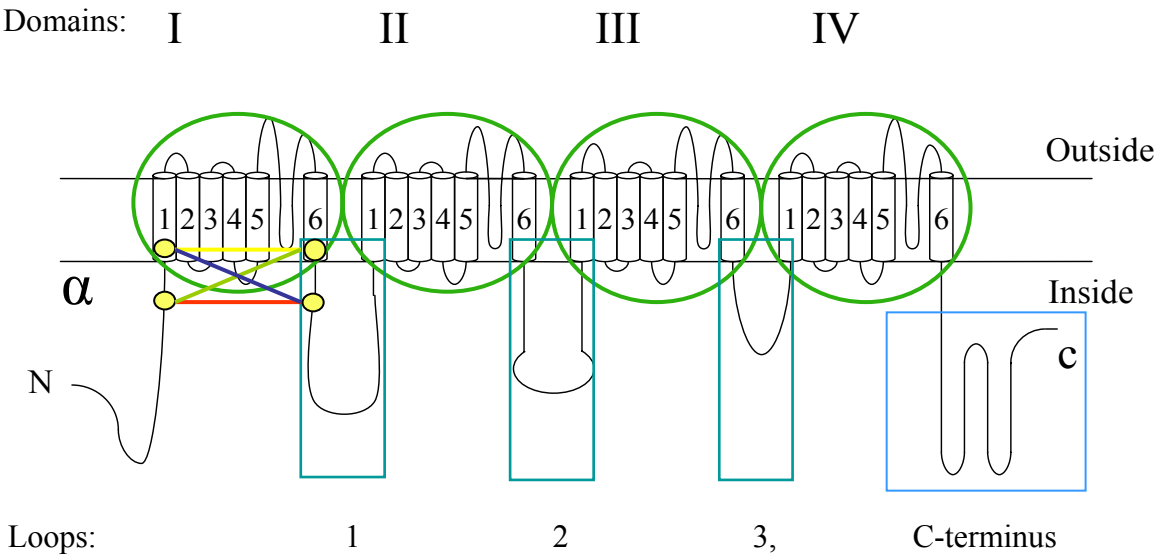

Fig. 10. Strategy of genetic research.
The schematic drawing shows structure of $Ca_V1.1$ channel. Two primer pairs were located close to exon-intron boundaries in every domain (marked with green circle), loop (marked with dark blue rectangle) and for C-terminus (marked with blue rectangle), to avoid overlooking of splicing variants. Primers are marked with yellow circles, amplification products are marked with colorful lines, red line indicates longest PCR product, yellow - shortest PCR product, green and blue intermediate ones.

Loop 1

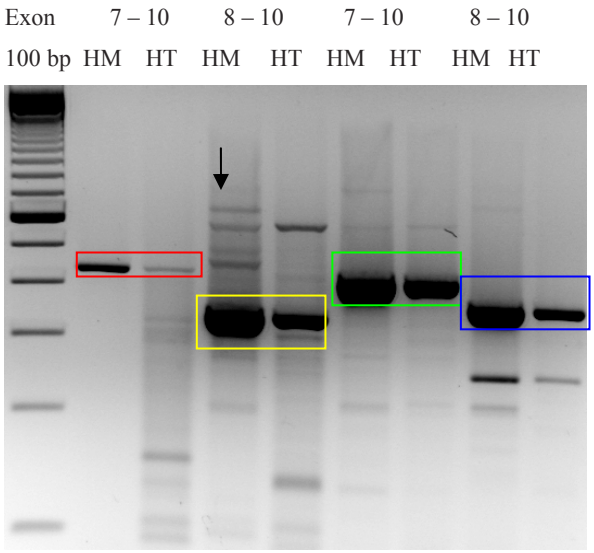

Loop 2

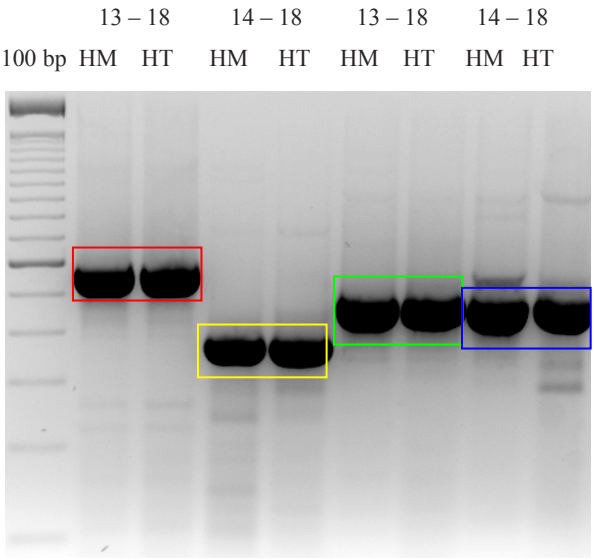

Loop 3

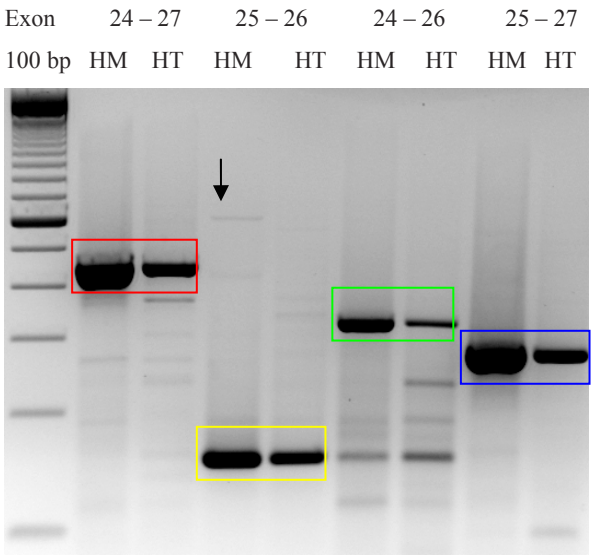

C-term

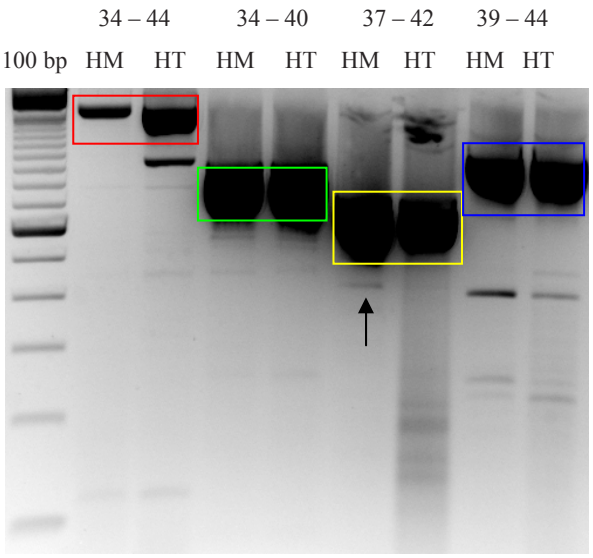

Fig. 11. Loops. RT-PCR with 2 pairs of primers placed in the neighborhood exons amplifying loop: 1, 2, 3 and C-terminus of *CACNA1S*, respectively. Red rectangle indicates longest PCR product, yellow - shortest PCR product, green and blue intermediate ones, as on Fig. 10.
Splice variant are marked with arrows, all other products are probably result of unspecific primers binding.
HM – human muscle and HT – myotubes

Domain I

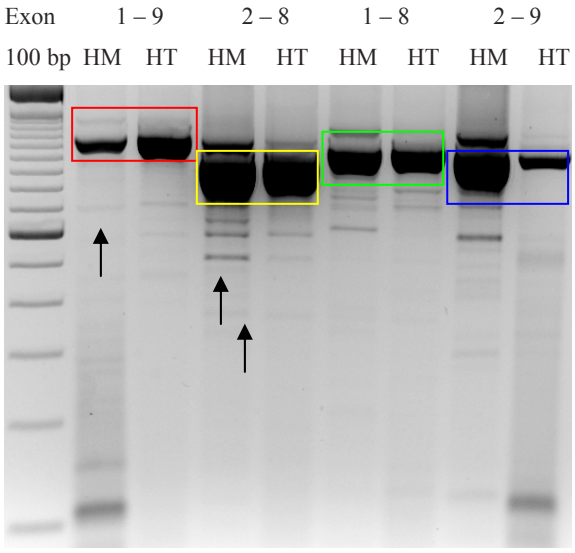

Domain II

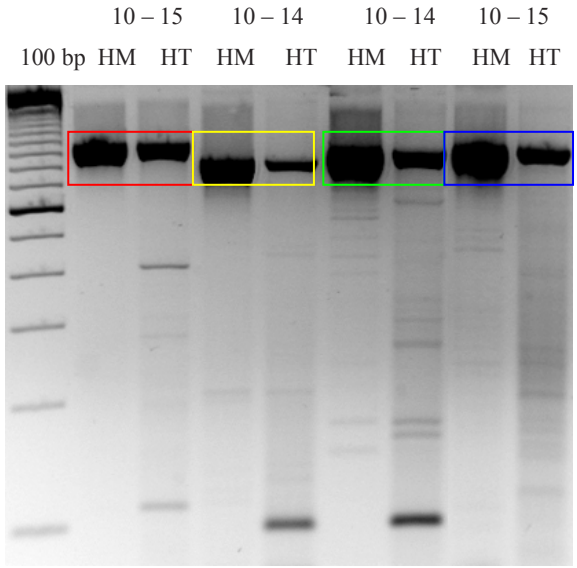

Domain III

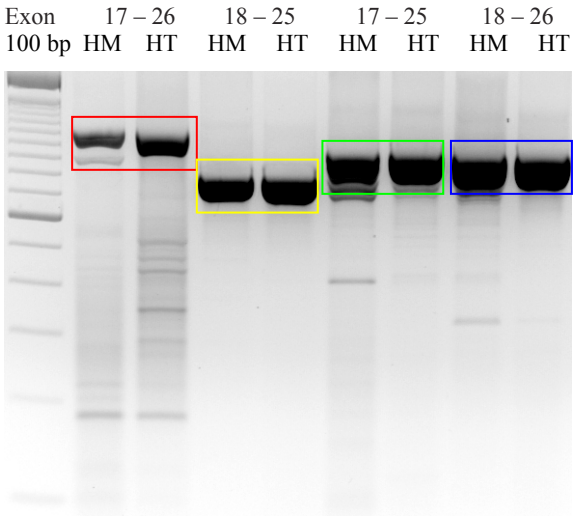

Domain IV

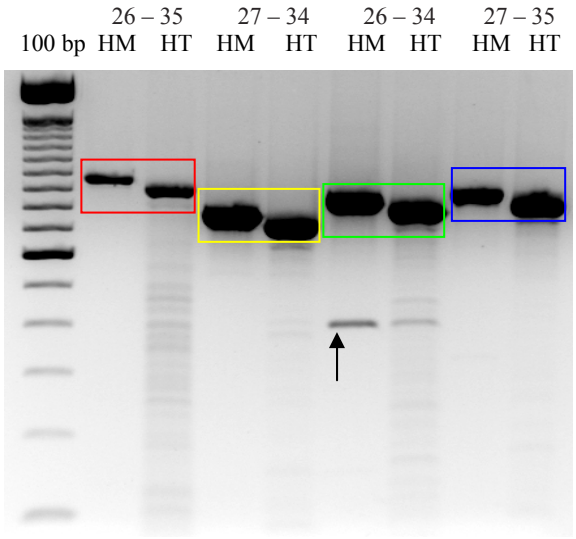

Fig. 12. Domains. RT-PCR with 2 pairs of primers placed in the neighborhood exons amplifying: domain: 1, 2, 3 and 4 of *CACNA1S* gene. Red rectangle indicates longest PCR product, yellow - shortest PCR product, green and blue intermediate ones, as on Fig. 10.
Splice variant are marked with arrows, all other products are probably result of unspecific primers binding.
HM – human muscle and HT – myotubes

III.1.2. Splicing variants in CACNA1S gene

Control muscle samples and myotubes cultured from them, were used for the analysis of alternative splicing in *CACNA1S* gene. Eight alternative variants were identified:

1. skipping of exon 3, 4 and 5 results in an early stop codon after 101 nonsense amino acids in IS3-4 (Fig. 13). This variant may be non-functional.

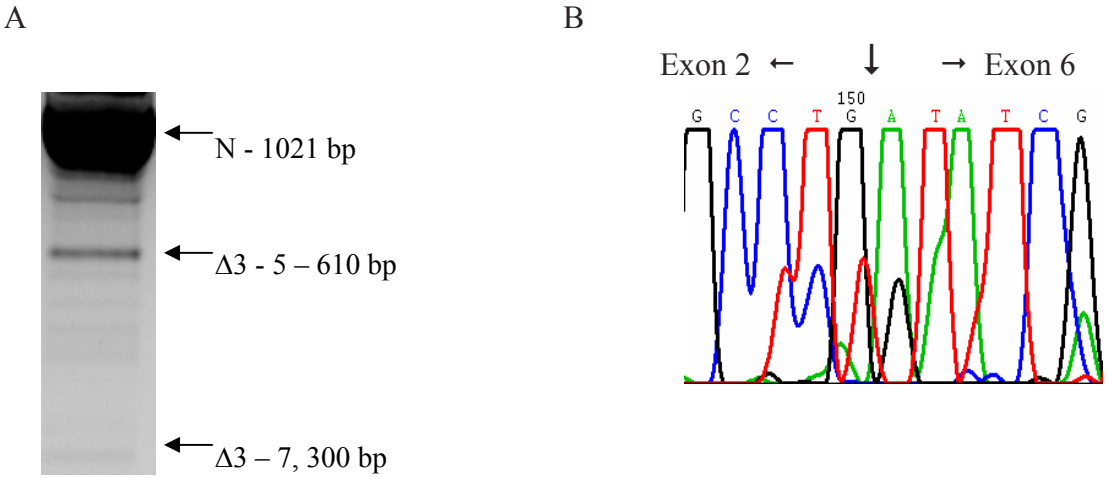

Fig. 13. (A) RT-PCR amplifying the region between exon 2 and 9 in *CACNA1S* gene.
(B) Sequencing chromatogram attesting skipping of exons 3, 4, 5

2. skipping of exon 3, 4, 5, 6 and 7 leads to early stop codon after 25 nonsense amino acids in IS3-4 (Fig. 14). It is probably not functional.

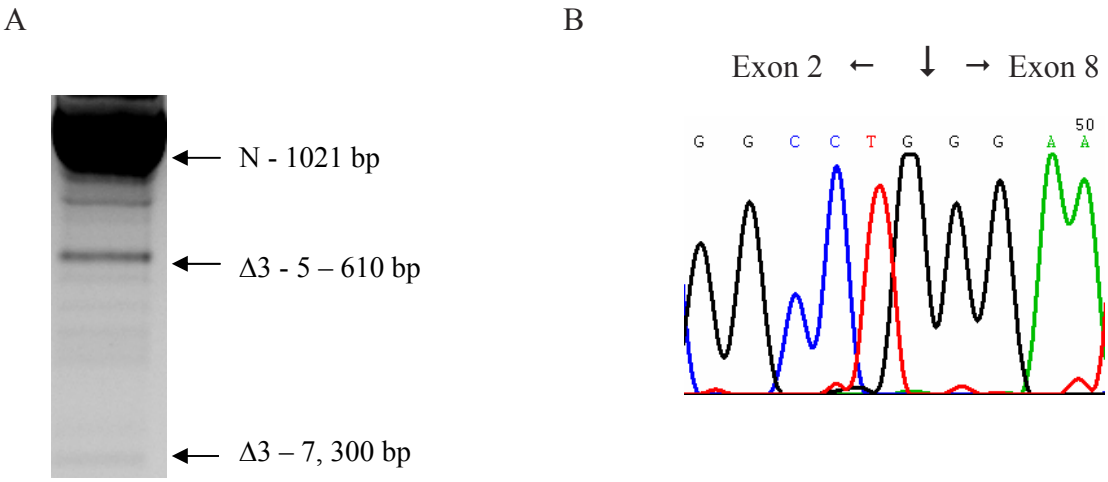

Fig. 14. (A) RT-PCR amplifying the region between exon 2 and 8 in *CACNA1S* gene.
(B) Sequencing chromatogram attesting skipping of exons 3, 4, 5, 6, 7

3. insertion of intron 4 results in an early stop codon at position 208 after 28 nonsense amino acids in IS4-5 (Fig. 15), it may be non functional.

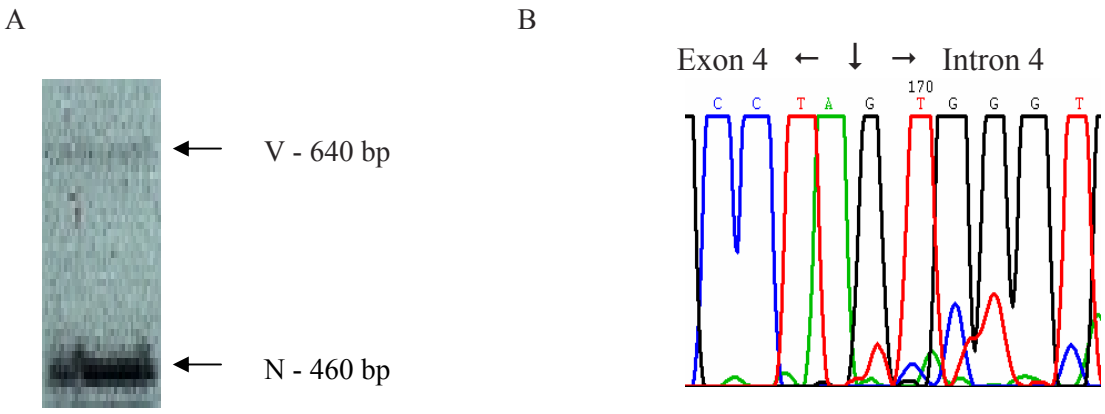

Fig. 15. (A) RT-PCR amplifying the region between exon 3 and 6 in *CACNA1S.* gene
(B) Sequencing chromatogram attesting insertion of intron 4

4. insertion of intron 8 leads to a stop codon after 78 amino acids in loop I-II (Fig. 16). Probably such truncated channel is not-functional.

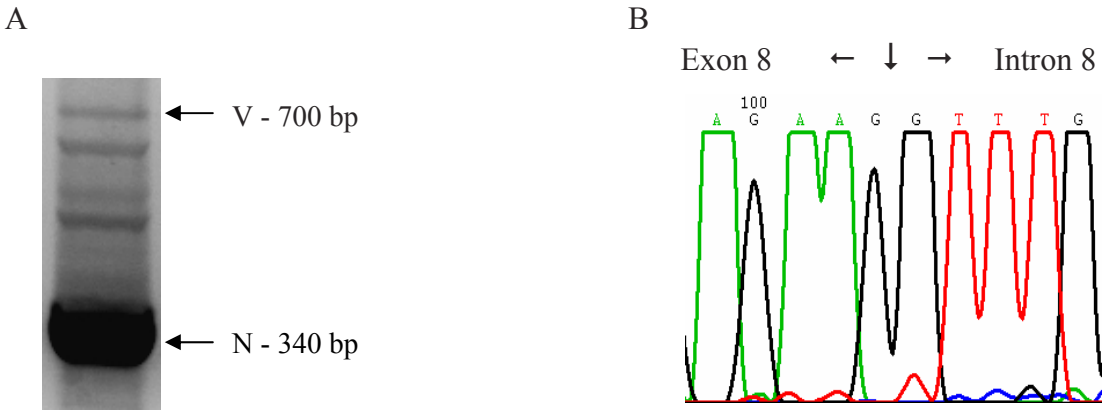

Fig. 16. (A) RT-PCR amplifying the region between exon 8 and 10 in *CACNA1S* gene.
(B) Sequencing chromatogram attesting insertion of intron 8

5. insertion of intron 25 causes early stop codon after 30 nonsense amino acids in loop III-IV (Fig. 17). This variant may be non-functional.

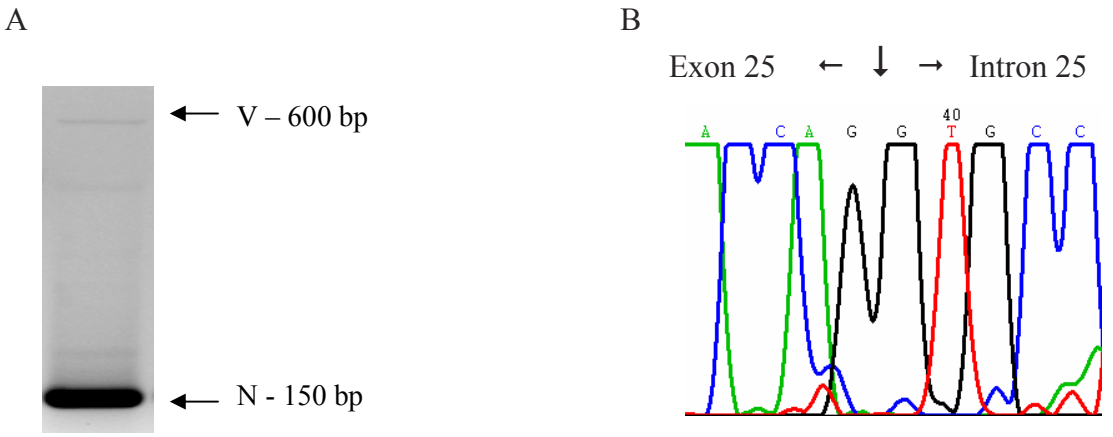

Fig. 17. (A) RT-PCR amplifying the region between exon 25 and 26 in *CACNA1S* gene.
(B) Sequencing chromatogram attesting insertion of intron 25

6. insertion of intron 26 results in 9 nonsense residues followed by an early stop codon at position 1138, located within IVS1 (Fig. 18), it may be non-functional.

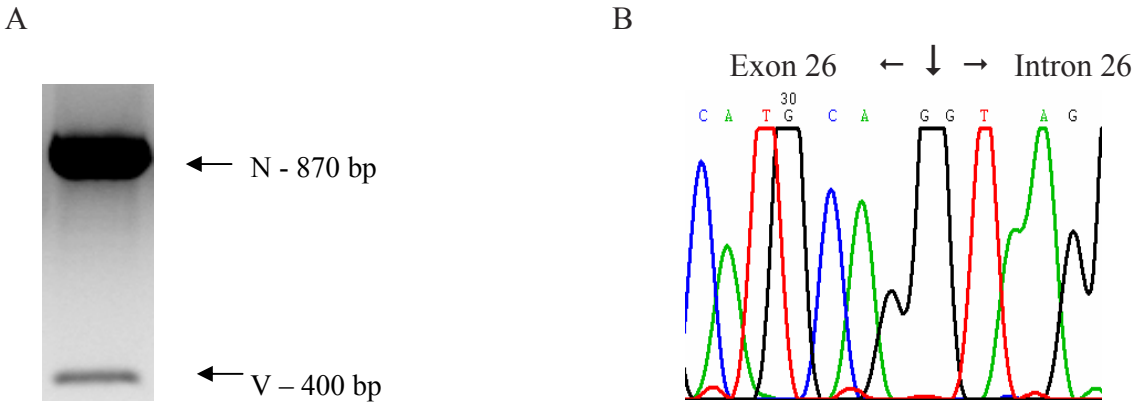

Fig. 18. (A) RT-PCR amplifying the region between exon 26 and 34 in *CACNA1S* gene.
(B) Sequencing chromatogram attesting insertion of intron 26

7. skipping of exon 29, leads to 19 amino acid deletion in extracellular IVS3-S4 loop (Fig. 19). This variant is dominant in myotubes and is functional. It was described previously in other species.

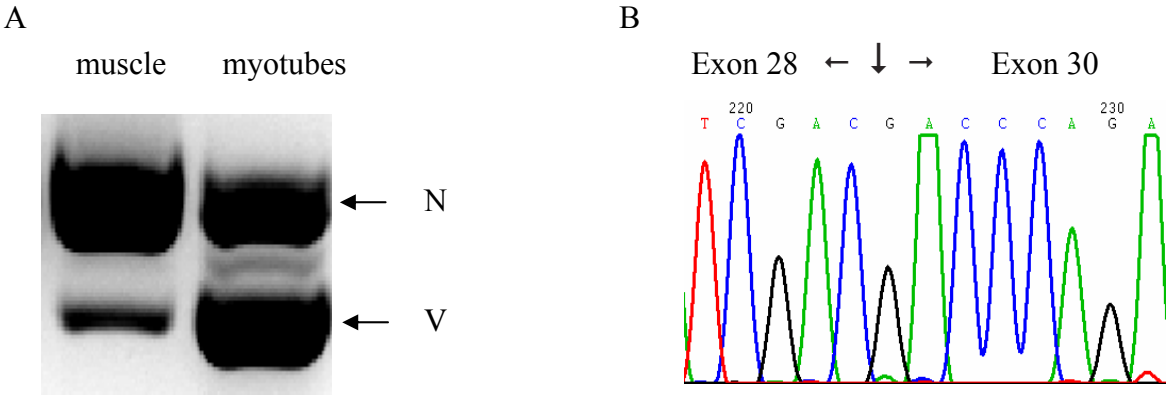

Fig. 19. (A) RT-PCR amplifying the region between exon 27 and 32 in *CACNA1S* gene.
(B) Sequencing chromatogram attesting skipping of exon 29

8. alternative 3' site of exon 40 deletes 78 nucleotides, without shifting of reading frame. It is located in the C-terminus (Fig. 20). This variant is probably functional.

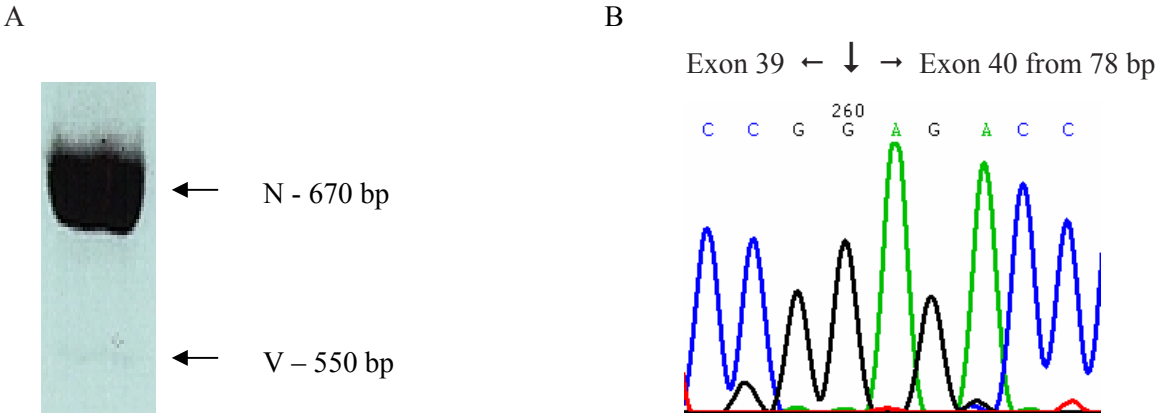

Fig. 20. (A) RT-PCR amplifying the region between exon 37 and 42 in *CACNA1S* gene.
(B) Sequencing chromatogram attesting alternative 5' end of exon 40

Table 3. Splicing variants in *CACNA1S* gene

Variant	DNA position in bp	Protein position and protein length (in aa)	Localization	% of transcripts
1. Deletion of exons 4, 5 *	398-694	132-231, 138	IS3-4	10
2. Deletion of exons 3, 4, 5	258-694	86-231 107	IS3-4	30
3. Deletion of exons 3 - 7	258-1004	86-335 101	IS3-4	17
4. Insertion of intron 4	At 541 additional 179 bp	At 180 208	IS4-5	24
5. Insertion of intron 8	At 1150 additional 404 bp	At 383 461	I-II	30
6. Deletion of exon 19 *	2490-2549	830-850 1853	IIIS2	14
7. Insertion of intron 25	At 3255 additional 450 bp	At 1085 1115	III-IV	36
8. Insertion of intron 26	At 3414 additional 1358 bp	At 1138 1147	IVS1	21
9. Insertion of intron 28 *	At 3609 additional 3845 bp	At 1203 1245	IVS3-S4	13
10. Deletion exon 29 *	3609-3666	1203-1222 1854	IVS3-S4	10 / 70
11. Alternative 3' site of exon 40	4797-4875	1599-1625 1847	C-term	15
12. Deletion of exon 39, 40 *	4668-5048	1556-1683 1600	C-term	16
13. Insertion of intron 43 *	At 5370 additional 148 bp	At 1790 1790	C-term	30

* This variants were described previously in our group (unpublished date).

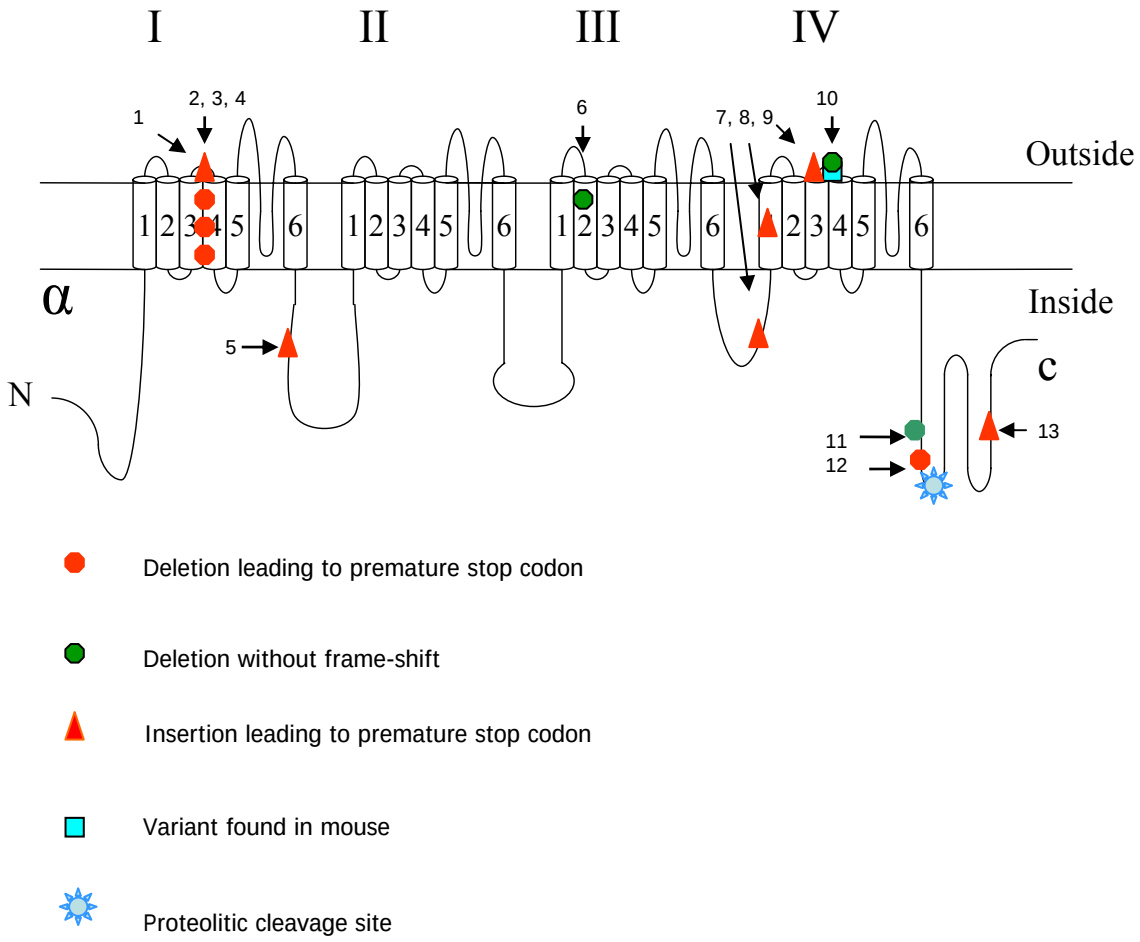

Fig. 21. 13 splicing variants found in the *CACNA1S* gene

Out of 13 splicing variants found in the *CACNA1S* gene, 4 are probably functional. Those are:

- Deletion of exon 19
- Deletion exon 29
- Alternative 3' site of exon 40
- Insertion of intron 43

It is crucial to continue investigation of splicing variants of $Ca_V1.1$ and to perform their functional characterization.

III.2. Gene expression

III.2.1. Expression of pEGFP- CACNA1Sh in TsA201 cells

Different transfection reagents and the calcium-phosphate method were used to express the pEGFP-CACNA1S fusion protein in TsA201 cells. We coexpress GFP-CANCA1Sh alone, or with auxiliary subunits (β_{1a} and $\alpha_2\delta$).The best results were obtained with Fugene 6.

High gene expression led to cell death, probably because the human $Ca_V1.1$ channel was "leaky", what cause Ca^{2+} overload of the cell and cytotoxicity, however, this remains to be proven. Low expression was undetectable, because of low fluorescence intensities. In consequence of these difficulties GLT cells were used for further investigations.

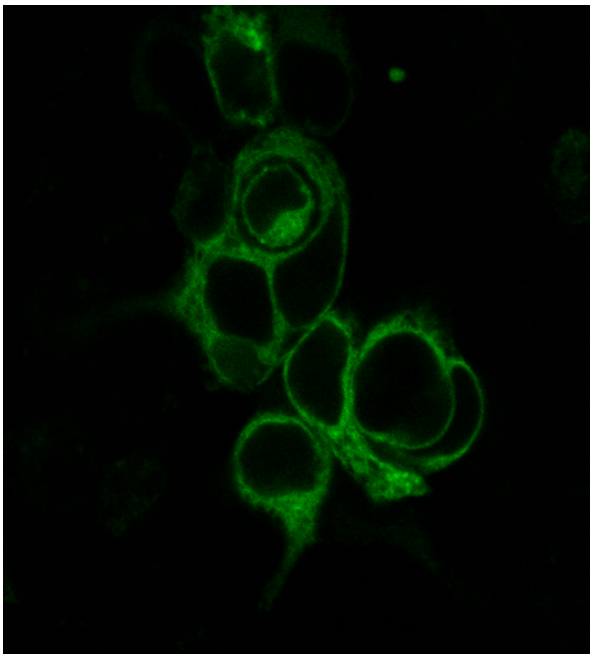

Fig. 22. TsA201 cells transfected with pEGFP-CACNA1Sh, showing channel expression in outer membrane. Expression level was highest at day 2.

III.2.2. Expression of plasmid pEGFP- CACNA1Sh in GLT cells

GLT cells were transfected at the onset of fusion (day 4) with Fugene 6. To prove proper targeting and incorporation of the calcium channel into junctions opposite to the RyR1, immunofluoroscence labelling was performed. Anti-GFP labelling showed a cluster

distribution pattern typical for triad proteins in skeletal muscle. The CACNA1S clusters showed a high degree of colocalization with the clusters of RyR1 (Fig. 23), a prerequisite for EC-coupling and calcium transients measurements.

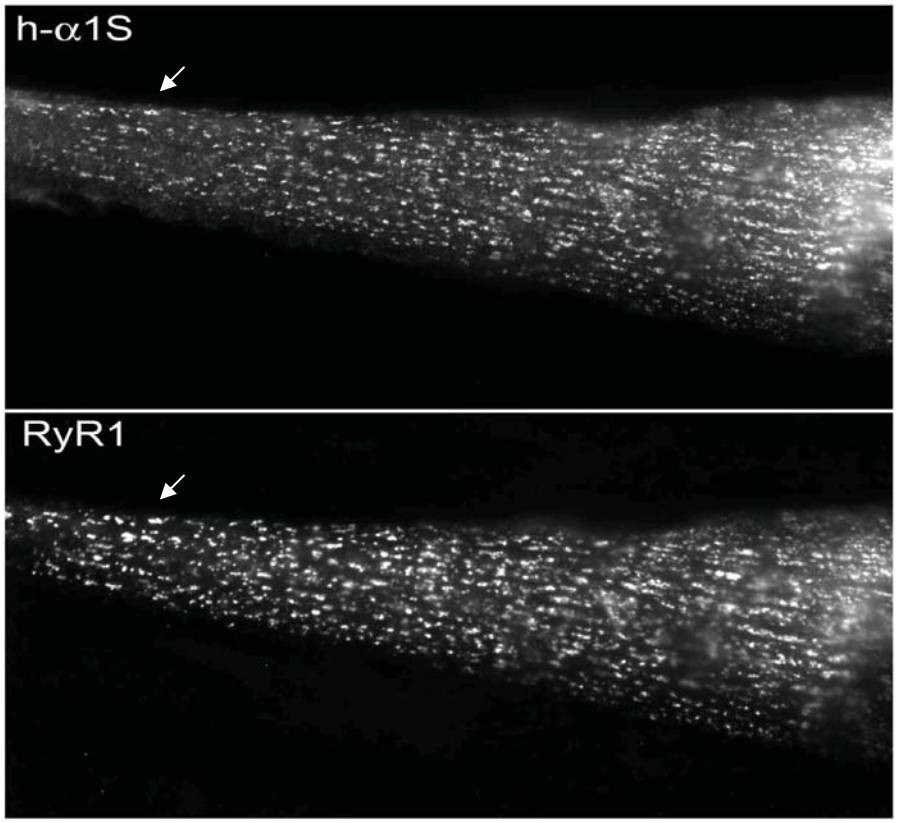

Fig. 23. Immunofluoroscence labeling. GLT cells were transfected with the human calcium channel pEGFP- CACNA1Sh. Double immunofluoroscence labeling with anti-GFP and anti-RyR1 as independent triad marker. The α_{1S} subunit is colocalized with RyR1 in clusters corresponding to triad junction (examples indicated with arrows).

The functional significance of truncated human CACNA1S expressed in GLT cells was investigated by patch clamp studies. As a positive control, a plasmid containing the rabbit calcium channel pGFP- CACNA1Sr was used, which is well described in literature. Calcium currents were evoked by applying of 200 ms voltage pulses between –50 and +80 mV in 10 mV increments. Representative current traces are shown on Fig. 24. Cells transfected with pGFP- CACNA1Sr exhibit well distinguishable currents. In contrast, transfection with pEGFP- CACNA1Sh showed much smaller currents (in average 0,3 pA/pF). In parallel to the currents we measured the calcium transients produced by $Ca_V1.1$ and the RyR1 interaction. In cells transfected with GFP- CACNA1Sr as soon as the membrane was depolarized, the intracellular calcium concentration raised ($\Delta F/F_0 = 1.6$). On the contrary human $Ca_V1.1$ gives no detectable calcium transients (Fig. 24), although a

very small current could be observed (which indicates that the channels are inserted into membrane and functional). Probably interaction between human $Ca_V1.1$ and the RyR1 was missing. Because human pEGFP- CACNA1Sh showed very small currents and no characteristic EC coupling we decided to use rabbit GFP- CACNA1Sr in further experiments.

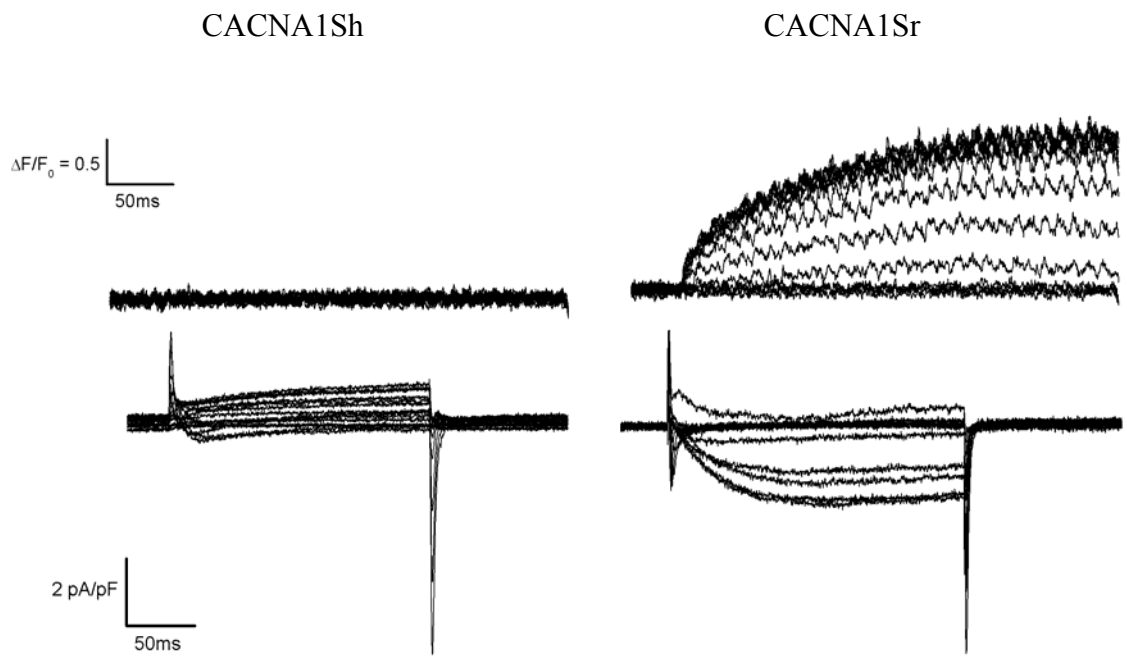

Fig. 24. Depolarization induced calcium transients (upper traces) and whole cell calcium currents (lower trace) recorded simultaneously from GLT cells expressing human pEGFP-CACNA1Sh (left site) and pGFP- CACNA1Sr (right site). The holding potential was -80 mV and 200 ms test pulses to potentials between -50 and +80 mV were applied in 10 mV increments. Changes in cytoplasmic free $[Ca^{2+}]$ were measured with Fluo-4 and shown as ($\Delta F/F$).

III.3. Combined whole cell patch clamp and intracellular fluorescence Ca^{2+} measurements

Combined whole cell patch clamp and intracellular fluorescence Ca^{2+} measurements were performed in transfected GLT myotubes loaded with the fluorescent Ca^{2+} indicator Fluo-4. Fig. 25 shows representative examples of recordings from GLT myotubes transfected with GFP-CANCA1Sr (control) or GFP-CANCA1SrΔ29.

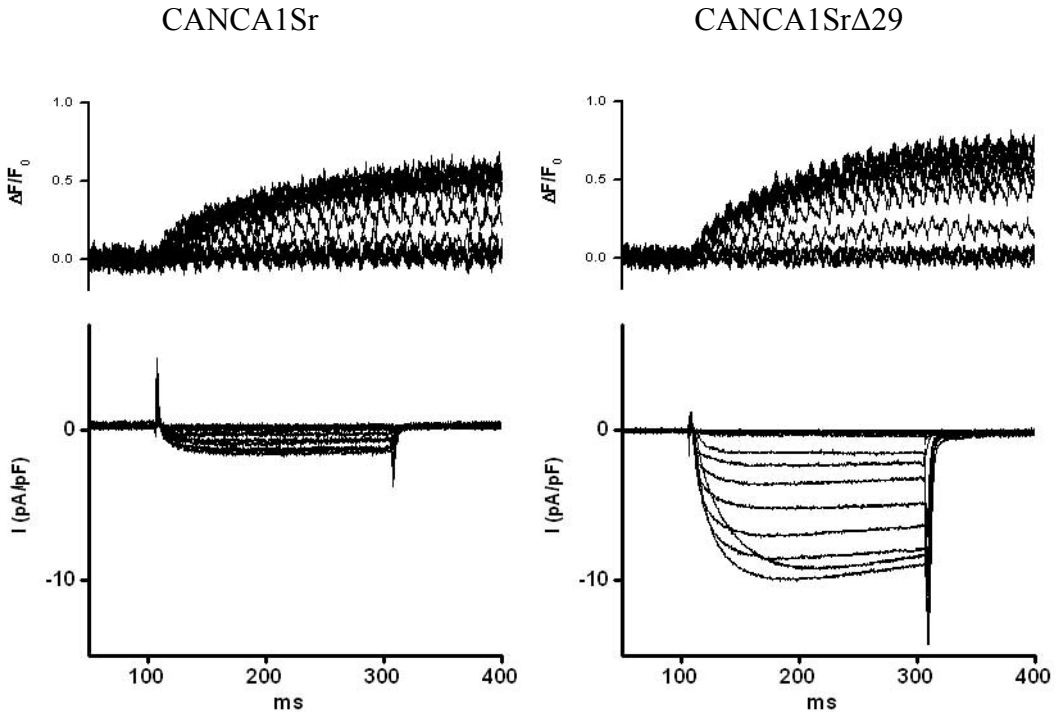

Fig. 25. Depolarization induced calcium transients (upper traces) and whole cell calcium currents (lower trace) recorded simultaneously from GLT cells expressing GFP-CANCA1Sr (left site) or GFP-CANCA1SrΔ29 (right site). The holding potential was -80 mV and 200 ms test pulses to potentials between -50 and +80 mV were applied in 10 mV increments. Changes in cyotoplasmic free [Ca^{2+}] were measured with Fluo-4 and shown as (ΔF/F).

III.3.1. Activation Properties of $Ca_V1.1$ Currents

Current properties of GFP-CANCA1Sr and GFP-CANCA1SrΔ29 were clearly different.

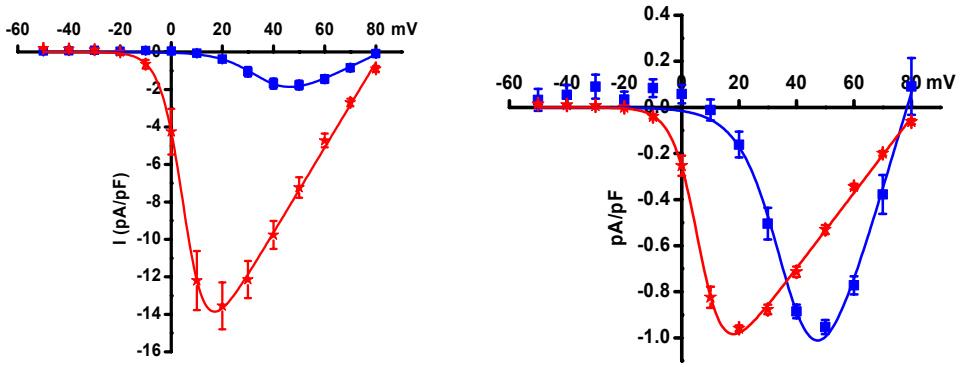

Fig. 26. Voltage dependence of Ca^{2+} currents. Maximum amplitude of the Ca^{2+} current plotted as a function of membrane holding potential. *Left* indicates a massive increase in the current amplitude while the normalized currents (*right*) clearly shows the shift in the voltage dependence of activation. Wild type is marked with blue color, variant with red color.

Dysgenic myotubes reconstituted with GFP-CANCA1Sr show an average current amplitude of -1.8 ± 0.25 (pA/pF) (n 15), while the GFP-CANCA1SrΔ29 expressing myotubes have an average current amplitude of -14.8 ± 1.37 (n 19) thus the lack of E29 increased the current amplitude by more then 8 times. The $V_{1/2}$ for WT was 39,2 ± 2,1 mV and variant demonstrated a shift by 32,5 mV in hyperpolarized direction (6,7 ± 1,2). The slope of voltage dependence of activation was also significantly altered. The reversal potential for both was similar (Table 4).

Compared to the control, the myotubes transfected with GFP-CANCA1SrΔ29 exhibited a 306% increase in the maximum conductance G_{max} (nS/nF).

III.3.2. Calcium transients

Depolarization induced intracellular calcium transients were measured during whole-cell recordings by including Fluo-4 in the pipette solution. The voltage dependence of calcium transients are displayed in Fig. 27 and show no significant difference between control and CANCA1SrΔ29- transfected myotubes. Depolarization to potentials between -50 mV and + 80 mV induced robust Ca^{2+} transients with a maximum $\Delta F/F$ of 0.51 ± 0.06 (GFP-CANCA1Sr, n=12) and 0.68 ± 0.08 (GFP-CANCA1SrΔ29, n=12).Voltage at half activation ($V_{1/2}$) was changed to more negative values, shifting the voltage dependence of activation to the left by about 8 mV for GFP-CANCA1SrΔ29. There was also change in steepness parameter.

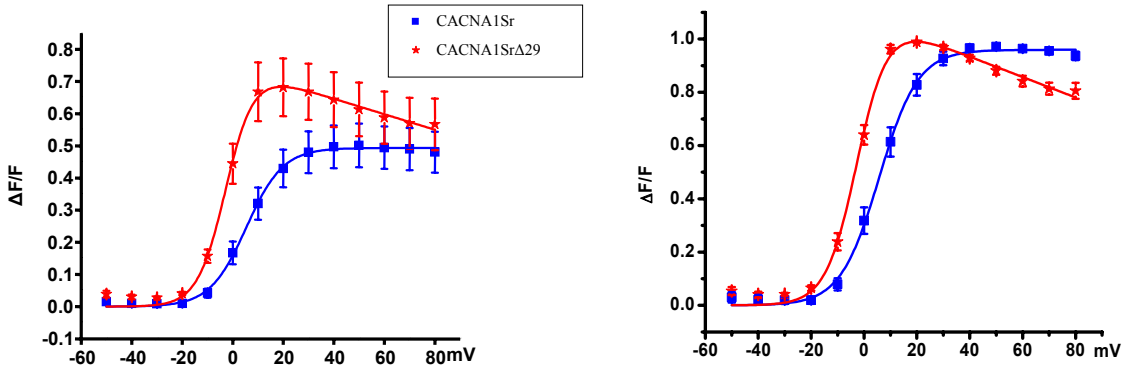

Fig. 27. Voltage dependence of the Ca^{2+} transients. The value of the ΔF/F was estimated by calculating the average over 50 ms at the end of the pulse. Left the absolute values, right the voltage dependence of normalized Ca^{2+} transients. Wild type is marked with blue color, variant with red color.

III.3.3. Calcium currents kinetics

In order to reveal the changes in the properties of activation kinetics the maximum inward current was fitted with a double exponential function. In agreement with published kinetic analyses of wild type myocytes and myotubes (Avila and Dirksen 2000), a double-exponential function is necessary to adequately fit the control currents and results in extraction of the amplitudes (A_{fast} and A_{slow}) and time constants (tau_{slow} and tau_{fast}) for each component of the macroscopic current. In spite of a > 8-fold in difference current density, calcium currents in both cases exhibited similar relative contributions of fast and slow components.

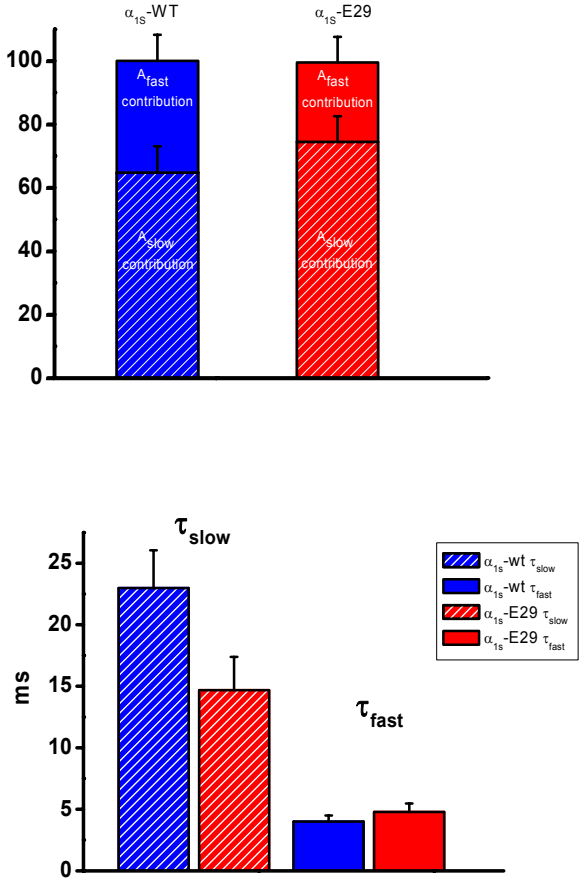

Fig. 28. Kinetic analysis of the Ca^{2+} currents show a slight modification of the time constants of activation indicating altered Ca^{2+} channel gating properties. The mean time constants for GFP-CANCA1Sr were τfast 3.9 ± 0.5 ms and τslow 22.9 ± 3.0 ms (Table 4); the mean current amplitudes Afast and Aslow were 1.1 ± 0.2 and 1.4 ± 0.4 pA/pF respectively. Thus, the relative contributions to the current amplitude were 35% for the fast and 65% for the slow component. The mean time constants for GFP-CANCA1S Δ29 were τfast 4.7 ± 0.6 ms and τslow 14.8 ± 2.4 the mean current amplitudes Afast and Aslow were 5.1 ± 1.2 and 13.8 ± 2.4 pA/pF respectively. Relative Afast/Aslow was 26/75%. According to Obermair et al. 2005, the two components of activation represent channels with and without the auxiliary subunit $\alpha_2\delta$-1. The deletion of exon 29 does not alter the association of the α_1 subunit with the $\alpha_2\delta$-1 subunit (the contribution of the two components to the total current amplitude is similar) but the time constants of activation were decreased indicating a faster gating of the Ca^{2+} channels.

Table 4. Properties of intracellular Ca^{2+} transients and Ca^{2+} currents from *CACNA1Sr* and *CACNA1SrΔ29* -transfected dysgenic myotubes were determined from combined whole cell patch clamp and intracellular Fluos-4 Ca^{2+} recordings as described in Materials and methods. Average values (±SEM) were obtained by fitting each myotube within a group separately to the appropriate equation.

	Parameters	CACNA1Sr-WT	CACNA1Sr-Δ29	Significance (p value)
Current properties	I_{peak} *(pA/pF)*	-1.8 ± 0.25	-14.8 ± 1.37	<0.001
	G_{max} *(nS/nF)*	75.3 ± 9.8	230.7 ± 17.9	<0.001
	$V_{1/2}$ *(mv)*	39.2 ± 2.1	6.7 ± 1.2	<0.001
	k_{act} *(mv)*	6.9 ± 0.4	4.0 ± 0.3	<0.001
	V_{rev} *(mv)*	83.5 ± 3.3	82.1 ± 0.5	ns
	n	15	19	-
Kinetics	A_{slow} *(pA/pF)*	1.4 ± 0.4	13.8 ± 2.4	<0.001
	A_{fast} *(pA/pF)*	1.1 ± 0.2	5.1 ± 1.2	0.003
	A_{slow} *contribution*	65%	75%	ns
	A_{fast} *contribution*	35%	26%	ns
	τ_{slow} *(ms)*	22.9 ± 3.0	14.8 ± 2.4	ns
	τ_{fast} *(ms)*	3.9 ± 0.5	4.7 ± 0.6	ns
	n	11	19	
Transients	*ΔF/F*	0.51±0.06	0.68 ± 0.08	ns
	$V_{1/2}$ *(mv)*	6.3 ± 1.9	-2.2 ± 0.9	<0.001
	k_{act} *(mv)*	6.9 ± 0.43	5.5 ± 0.25	0.01
	n	12	12	-

All data are presented as mean ± S.E.M.
ns - indicates non significant
n - number of tested celles

IV. DISCUSSION

IV.1. Splicing variants in C-terminus of $Ca_V1.1$

In the region coding for C-terminus we identified a splice variant, which causes premature termination by insertion of intron 43 at position 1790 amino acids (aa). In this case, many consensus sites for cAMP-dependent protein phosphorylation, which are present in the distal C-terminal region of α_1 will be lost. They may be important for the regulation of the ion conductance activity of the calcium channel (De Jongh et al. 1991). In vivo, the splice variant is proteolyticaly cleaved near amino acid residue 1685, just like the most of full length product (De Jongh et al.1991). However, the cleaved C-terminus cannot reassociate with the proximal part of channel, because the interaction site at 1802–1841 aa is missing. Hulme et al. (2005) proved that the proteolytically processed distal C-terminus of rabbit $Ca_V1.1$ is noncovalently associated with the remainder of the channel via an interaction with a site in the proximal C-terminal domain (1556–1612 aa) when expressed as a separate protein in mammalian non-muscle cells. Artificial truncation of the rabbit $Ca_V1.1$ channel at position 1698 aa significantly increases the magnitude of gating charge movements and supported much larger ionic currents (Morrill and Cannon 2000). This suggests that the C-terminus of $Ca_V1.1$ may play a role in channel expression in the membrane as well as in the coupling of gating to pore opening. Our variant may show a similar functional effect.

We analyzed the sequences of human Ca_V1 subfamily (Fig. 29) and found that two other C-terminus variants: alternative 3' site of exon 40 (protein length - 1847 amino acids) and deletion of exon 39, 40 (1600 aa), which we found, could have a comparable effect. The proximal C-terminal interaction domain (PCID 1556–1612 aa) is encoded by exon 39 and beginning of exon 40 (Fig. 29). In case of exon 39, 40 deletion the PCID region is completely gone, followed by premature stop codon. In the variant with alternative 3' site of exon 40 the reading frame is not shifted, however, the cleaved C-terminus can not associate with channel because the PCID region is partly gone.

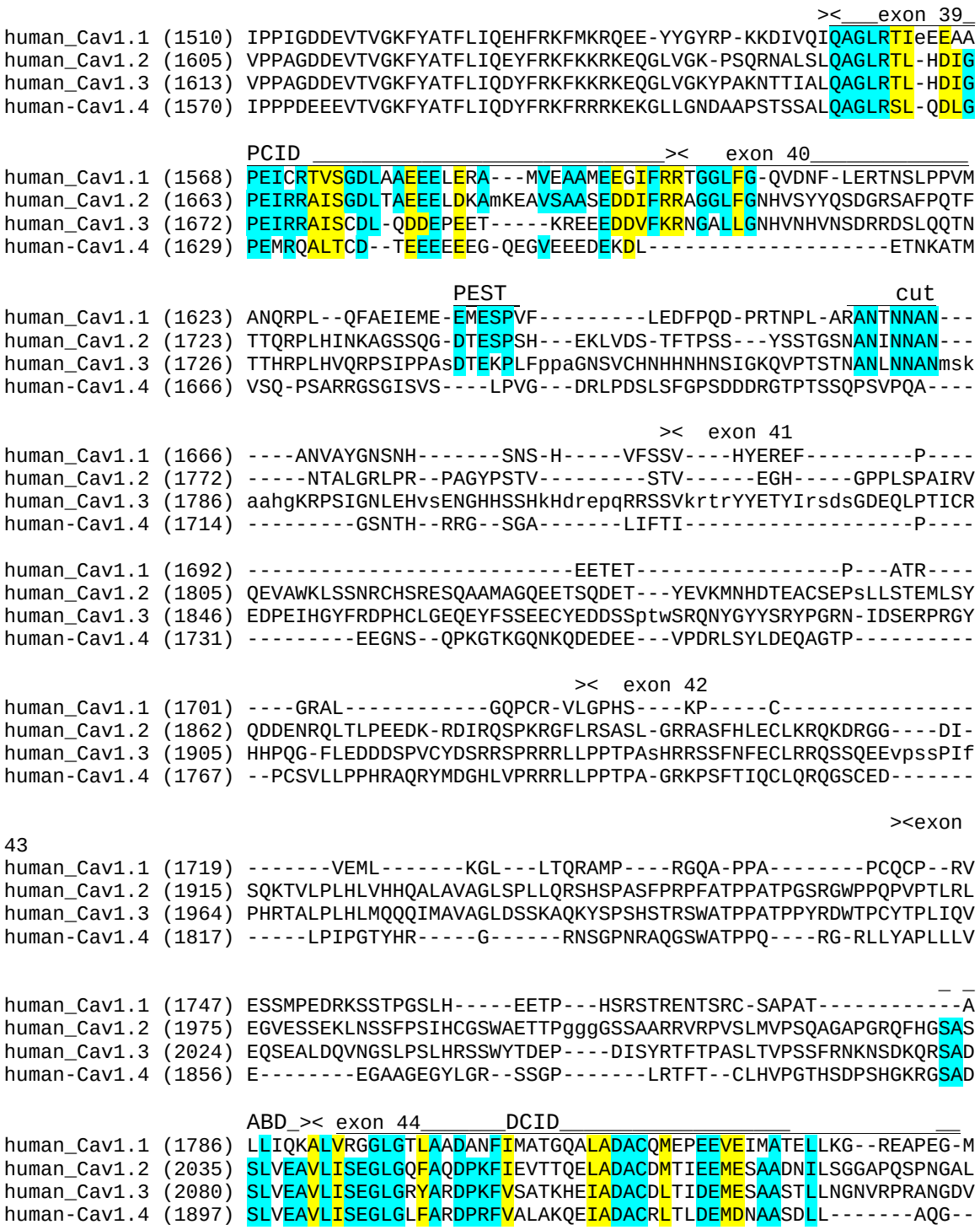

Fig. 29. Conserved amino acid sequences of Ca_V1 subfamily at the sites of C-terminal interaction and proteolytic cleavage. Amino acid sequence alignment of the proximal C-terminal interaction domain (PCID), distal C-terminal interaction domain (DCID), proteolytic signal to target proteins for degradation (PEST motif), the proteolytic cleavage site (cut), and the AKAP15-binding domain (ABD) identified in human: $Ca_V1.1$ with $Ca_V1.2$, $Ca_V1.3$, and $Ca_V1.4$. Conserved amino acids are shaded in blue, and similar amino acids are shaded in yellow. Borders between exons are marked ><.

C-term in vivo proteolysis is also found in other channels, for example $Ca_V1.2$ channels in heart and brain are also truncated at a similar position in their C-terminus (De Jongh et al. 1994). Expression of $Ca_V1.1$ and $Ca_V1.2$ channels with truncated C-terminus in Xenopus oocytes (Ivanina et al. 2000, Morrill and Cannon 2000) or TsA-201 cells (Kepplinger et al. 2000, Geo et. 2001) increases the functional activity of these channels, suggesting that the distal C-terminus has an autoinhibitory effect. In addition it has also been reported that $Ca_V1.3$ (Hell et al. 1993), $Ca_V2.1$ (Kubodera et al. 2003), and $Ca_V2.2$ (Westenbroek et al. 1992) are cleaved in neurons. This suggests that C-terminal cleavage is a general feature of Ca_V channels. Hulme et al. (2006) reported that formation of the autoinhibitory complex in $Ca_V1.2$ greatly reduces the coupling efficiency of voltage sensing to channel opening and shifts the voltage dependence of activation to more positive membrane potentials. It is possible that for $Ca_V1.3$, the interaction of distal and proximal C-terminus sites forms an autoinhibitory module for voltage-dependent facilitation (VDF) which is disrupted when the distal C-terminus is removed by alternative splicing in $Ca_V1.3$ (Calin-Jageman et al. 2007). Those results suggest that $Ca_V1.1$, $Ca_V1.2$ and $Ca_V1.3$ are truncated by proteolytic processing to produce an autoinhibited channel complex. We can expect that splicing variants in C-terminus will lack this autoinhibitory mechanism and in consequence show larger, more rapid currents and increased gating charge movements.

Lack of distal C-terminus not only changes $Ca_V1.1$ function, it can also regulate transcription. Gomez-Ospina et al. (2006) showed that truncated C-terminus of $Ca_V1.2$ binds to a nuclear protein, associates with an endogenous promoter, and regulates the expression of a wide variety of endogenous genes important for neuronal signalling and excitability. This process is regulated both developmentally and by changes in intracellular calcium. Also Kordasiewicz et al. (2006) demonstrate that the C-terminus of $Ca_V2.1$ is cleaved from the full-length protein and translocated to the nucleus. These findings provide evidence that voltage-gated calcium channels can directly activate transcription and suggest a mechanism linking voltage-gated channels to the function and differentiation of excitable cells.

IV.2. Splicing variants in first domain

Most of the splicing variants, which we found, are located in domain I region, or shortly after it (Table 3). Those are: deletion of exons 4, 5 (protein length - 139 amino acids), deletion of exons 3, 4, 5 (187 aa), deletion of exons 3 – 7 (111 aa), insertion of intron 4 (208 aa) and insertion of intron 8 (461 aa). All of them insert premature termination codons in the first domain and would not generate a functional channel protein by themselves. This could have three different consequences for $Ca_V1.1$ channel: nonsense-mediated decay (NMD), leaky ribosomal scanning, or dominant-negative calcium channel suppression. The first case is the most probable one, because as many as one third of alternative splicing events insert premature termination codons that usually result in mRNA degradation by nonsense-mediated decay (Lewis et al. 2003), especially when termination codons are more than 50-54 nucleotides before the final exon-exon junction (Nagy and Maquat 1998). This mechanism of regulation of gene expression (Lewis et al. 2003, Cooper 2005) is also found in the homologous $Ca_V1.2$ channel. Exclusion of exon 9 together with 8 or 8a in I-II loop shifts the frame and introduce premature stop (Tang et al. 2004), that possibly give rise to NMD also.

Secondly, leaky ribosomal scanning may lead to restart of translation, at any subsequent start codon following the premature stop codon. In these cases, channel function may be recovered by expression of complementary protein fragments from the same cDNA. Such a case was described by Ahern et al. (2001), who characterized a single-base frame-shift mutant of $Ca_V1.1$. The frame-shift mutant expressed the N-terminal half of $Ca_V1.1$ (M1 to L670) and the C-terminal half starting at M701 separately. The C-terminal fragment was generated by an unexpected restart of translation at M701 and was eliminated by a M701I mutation. Protein-protein complementation between the two fragments (hemichannels) produced recovery of skeletal-type EC coupling but not $Ca_V1.1$ current. Flucher et al. (2002) studied the targeting properties of $Ca_V1.1$ two-domain fragments joined with green fluorescent protein (GFP) I·II (1–670) and III·IV (691–1873). Coassembly of the two complementary fragments formed a functional channel.

Thirdly, dominant-negative calcium channel suppression may result from the premature stop codons generated by alternative splicing. This mechanism of the suppression requires interaction between a variant with premature truncation and a related full-length channel. This interaction activates a component of the unfolded protein

response (UPR) to suppress translation (Page et al. 2004). The UPR is initiated when the endoplasmic reticulum (ER) lumen is unable to cope with the load of newly synthesized proteins requiring folding, as in homologues $Ca_V2.2$ channel. Coexpression of the truncated domain I of $Ca_V2.2$, together with full-length $Ca_V2.2$, reduced the level of $Ca_V2.2$ protein. Therefore, it is possible that some of $Ca_V1.1$ truncated variants which we found could suppress expression of full length $Ca_V1.1$.

In addition to the above, the variant with intron 8 insertion may form 2- or 4-domain channels by homomerization. Existence of two-domain calcium channel polypeptides has been reported, a two-domain, form of $Ca_V1.1$ comprising domain I and chimeric domain IV generated by splicing of the region encoding the S2 segment of domain II to the region encoding the S2 segment of domain IV has been observed predominantly in muscle from neonatal rabbits (Malouf et al. 1992). In $Ca_V2.1$ channels, a polypeptide that comprised domains I and II and a part of loop II-III was able to bind the auxiliary β subunits (Scott et al. 1998), and it remains to be determined whether the polypeptide can form functional channels. In homologous $Ca_V1.2$, Diebold et al. (1992) found 2 variants: truncated, two-domain polypeptides composed of normal domains I and II with premature truncations at different sites of the wild-type II-III loop.

IV.3. Premature truncations after third domain.

Three more splicing variants can produce premature truncations. Those are: insertion of intron 25 (protein length - 1115 amino acids), insertion of intron 26 (1147 aa) and insertion of intron 28 (1245 aa). All three variants introduce premature stop codons and probably form non-functional channels. Therefore, they could be subject to the same processes, as the variants in the first domain: NMD, leaky ribosomal scanning and dominant-negative calcium channel suppression.

IV.4. Splicing variant in third domain

In third domain we found just one variant: deletion of exon 19. It is probably functional, because the reading frame is not shifted, but it could behave differently than wild type $Ca_V1.1$, because 20 amino acids, which form most of IIIS2 segment are gone.

This region contains a dihydropyridine binding site (Soldatov et al. 1995), which is probably missing in this case. This area is also spliced in the homologous human $Ca_V1.2$ channel (corresponding exons 21/22), which changes voltage dependence of dihydropyridine action (Soldatov et al. 1995, Zuhlke et al 1998).

The second important function of the S2 segment is its contribution to voltage sensing. Due to the conservation of domain structure between channels transporting different cations, the contribution of the S2 segment to voltage sensing shown in potassium channels also applies to the Ca_V family. Shaker potassium channel have a potential voltage-sensing residue in S2 (E293) neutralization of which has effects on gating charge comparable to any single S4 mutation (Seoh et al., 1996). Two of the four potential voltage-sensing residues in Ca^{2+}-activated potassium channel are located in S2 (D153, R167). Other K_V channels also contain conserved acidic and basic residues at these positions that effect voltage sensing (Zhongming et al. 2006).

Alternative splicing in region encoding IIIS2 is age-dependent. Abernethy and Soldatov (2002) showed switch of the exon 22 to 21 isoform of $Ca_V1.2$ in human donors older than about 50 years. The splice variants are also tissue-dependent: the IIIS2 region of $Ca_V1.3$ shows a splice choice (exon 22a) that is associated with the hair cell organs of trout, chick, and rat (Ramakrishnan et al. 2002), but is not found in the brain (Kollmar et al. 1997).

This suggest that in case of exon 19 deletion some voltage sensing residues in S2 are gone, what can have effects on both S4 voltage sensitivity function and the voltage-dependent of inactivation by DHPs.

IV.5. Splicing variant in IVS3-S4 region

We found a deletion of exon 29 (Δ29) in human *CACNA1S* gene, leading to 19 amino acids shortening of the IVS3-S4 linker. A homologous variant has been described in mouse (Perez-Reyes et al. 1990). Similar variants of IVS3-S4 region are found in multiple calcium channel genes and many different species from *Drosophila* to human. This suggest a special significance of this splice site

Several IVS3-S4 variants of homologous channels have been functionally characterized. Addition of just two amino acids in the same linker region in the $Ca_V2.1$ and $Ca_V2.2$ channels showed altered biophysical and pharmacological properties (Bourinet et

al. 1999, Lin et al. 2004): insertion of the two residues NP by splicing in the IVS3-S4, showed a significant positive shift in the current–voltage relationship by ~6 mV. The second major change in channel properties associated with NP insertion is 11-fold decreased ω-Aga IVA (spider peptide toxin) affinity (Bourinet et al. 1999). In $Ca_V2.2$ an analogous variant, an ET insertion by splicing in the corresponding IVS3-S4 slows the speed of channel activation (Lipscombe et al. 2002) and slows gating, independent of expression system and of the presence of the $\alpha_2\delta$ auxiliary subunit (Lin et al. 2004). Steady-state voltage dependence of channel opening and of charge movement were not different between splice forms when expressed in mammalian cells.

The biggest variability in IVS3-S4 length was found in closest homolog $Ca_V1.2$ channel (Tang et al. 2004). There are 12 IVS3-S4 splicing combinations of $Ca_V1.2$, four of which were examined functionally: A (13 amino acids shorter IVS3-S4 loop), B (-6 aa), C (-11 aa), and D (12 of 28 aa IVS3-S4 loop are different). Whole-cell barium currents showed a $V_{1/2}$ for the WT of -9.3 ± 1.28 mV, while three splice variants (A, B, and C) demonstrated a shift in the I-V curve into the hyperpolarized direction. Variant A shifted $V_{1/2}$ by -9.5 mV (-18.8 ± 0.97 mV), B by -4.9 mV (-14.2 ± 0.60 mV), and C by -6.8 mV (-16.1 $\pm$ 0.86 mV). Nonetheless, the difference between the $V_{1/2}$ for the WT and D variant, that contained equal IVS3-S4 linker lengths, even though 12 of 28 amino acids were different, was not statistically significant.

In $Ca_V1.1$ we performed electrophysiological recordings of the IVS3-S4 splice variant in transfected GLT myotubes. Deletion of exon 29 in $Ca_V1.1$ removing 19 amino acids from IVS3-S4 region shifted the I-V curve of the variant by -32,5 mV (6.7 ± 1.2). Our results are nicely consistent with findings in other homologous calcium channels: there appears to be a correlation between the IVS3-S4 linker length of the variants and the amount of hyperpolarizing shift in the voltage dependence of activation when compared with the WT. This is evident in the large shift in the $V_{1/2act}$ by -10 to -11 mV for a deletion of 11–13 aa compared with a smaller shift of 5 mV for a 2 aa deletion in the IVS3-S4 linker (Tang et al. 2004). Similar results are also demonstrated for the shift in I-V relationships.

An important feature of IVS3-S4 variants is the specific tissue- and age-dependent expression. In the $Ca_V1.3$ exon 32 encoding the IVS3–4 loop is optional, it is inserted in hair cells, but not in the brain (Kollmar et al. 1997). In $Ca_V2.2$ ET insertion (cassette-exon 31a) in the IVS3-S4 loop is restricted to the peripheral nervous system (Lipscombe et al. 2002). The predominant splice combination in the $Ca_V1.2$ for the fetal heart and the fetal

and adult brain at the IVS3-S4 region is WT (-31, +32, and +33). There is, however, co-dominant isoform in the adult heart - variant C (-31, +32, and -33). Whereas on the other extreme, the variant A (-31, +32-6 nt, and -33) is detected at low levels representing between 1% in adult brain to 7% in adult heart. Variant B (-31, +32-6 nt, and +33) is expressed at a higher level 11-16% in all the samples. The 3-fold increase in variant C (-31, +32, -33) of adult (31%) over fetal (10%) heart could have arisen by developmental regulation of exon 33. Most interestingly, there is a 10-fold lower expression of variant C in adult brain when compared with adult heart pointing to a tissue or physiological difference in expression (Tang et al. 2004). These results are nicely consistent with our findings, namely, expression of $Ca_V1.1$ without exon 29 is much higher in myotubes (70%) than in adult muscle (10%). We have obtained similar results with mouse myotubes (C_2C_{12}) and mouse muscle (Fig. 30). We can speculate that Δ29 channels would activate upon slight membrane depolarization, resulting in early onset or increased frequency of contraction of muscle immediately after the arrival of a depolarizing pulse.That is why it is not recommended to use cultured cells as a model of adult muscle in electrophysiological experiments.

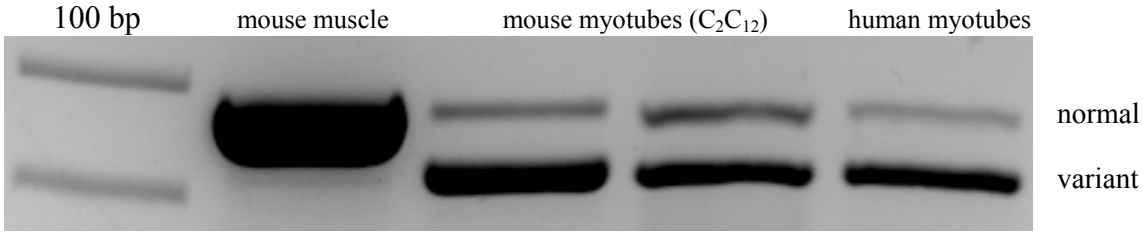

Fig. 30. RT-PCR amplifying the region between exon 27 and 32 in *CACNA1S* gene.

Alternative splicing of exon 29 appears to underlie the key shift in voltage parameters. Our research provided valuable evidence on the dominant expression of Δ29 channels in neonates and regenerative muscles. It also provided further evidence for phenotypic variation generated by alternative splicing to produce proteomic diversity.

V. SUMMARY

Alternative splicing is likely to be the primary source of human proteomic diversity. Our aim was to investigate the splice variants of the human *CACNA1S* gene. The encoded voltage-gated calcium channel $Ca_V1.1$ is mostly expressed in skeletal muscle cell, where it controls the activity of intracellular calcium realize channel RyR1, during excitation-contraction coupling. We extracted RNA from human muscle and human myotubes cell culture, performed reverse-transcriptase PCR and direct sequencing of all variants found. We identified 13 different splice variants: 9 generating premature truncations and 4 generating putatively functional channels. Premature truncation could have three different consequences for $Ca_V1.1$ channel: nonsense-mediated decay (NMD), leaky ribosomal scanning, or dominant-negative calcium channel suppression.

We focussed on splice variant excluding exon 29 (Δ29). This region codes most of IVS3-S4 loop. The IVS3-S4 region is subjected to extensive splicing in multiple calcium channels genes and different species from *Drosophila* to human. Variant without exon 29 is highly expressed in human and mouse myotubes (~70% of transcripts) but relatively rare in adult muscle (~10% of transcripts). For this reason, we undertook functional studies of this variant. Experiments with plasmid containing human *CACNA1S* did not give satisfactory results. Expression in TsA201 cells caused cytotoxicity and cell death. Transfection of GLT cells were successful, we measured small cell currents, but no detectable calcium transients. We decided to use rabbit *CACNA1S* in further experiments. Combined whole cell patch clamp and intracellular fluorescence Ca^{2+} measurements were performed in transfected GLT myotubes loaded with the fluorescent Ca^{2+} indicator Fluo-4. Current kinetics of wild type and Δ29 were clearly different, the I-V curve of the variant was -32 mV shifted. Our results are nicely consistent with findings in other homologous calcium channels: there appears to be a correlation between the IVS3-S4 linker length of and the amount of hyperpolarizing shift in the voltage dependence of activation when compared with the WT. Compared with control myotubes, myotubes transfected with Δ29 exhibited a 300% increase in the maximum conductance G_{max} (nS/nF).

Alternative splicing of exon 29 appears to underlie the key shift in voltage parameters. Our research provided valuable evidence on the dominant expression of Δ29 channels in neonates and regenerative muscles. It also provided further evidence for phenotypic variation generated by alternative splicing to produce proteomic diversity.

VI. REFERENCES

1. Abernethy D.R., Soldatov N.M. 2002. Structure-Functional Diversity of Human L-Type Ca2+ Channel: Perspectives for New Pharmacological Targets. J. Pharmacol. Exp. Ther. 3: 724-8.

2. Ahern C.A., Vallejo P., Mortenson L., Coronado R. 2001. Functional analysis of a frame-shift mutant of the dihydropyridine receptor pore subunit (α1S) expressing two complementary protein fragments. BMC Physiol. 1: 15.

3. Arikkath J., Campbell K.P. 2003. Auxiliary subunits: essential components of the voltage-gated calcium channel complex. Curr Opin Neurobiol. 3: 298-307.

4. Avila G, Dirksen RT. 2000. Functional impact of the ryanodine receptor on the skeletal muscle L-type Ca(2+) channel. J Gen Physiol. 4: 467-80.

5. Bean BP. 1989. Classes of calcium channels in vertebrate cells. Annu Rev Physiol. 51: 367-84.

6. Black D.L. 2003. Mechanisms of alternative pre-messenger RNA splicing. Annu Rev Biochem. 72: 291-336.

7. Blencowe B.J. 2006. Alternative splicing: new insights from global analyses. Cell. 126(1): 37-47.

8. Blumenstein Y., Kanevsky N., Sahar G., Barzilai R., Ivanina T., Dascal N. 2002. A novel long N-terminal isoform of human L-type Ca2+ channel is up-regulated by protein kinase C. J Biol Chem. 5: 3419-23.

9. Bourinet E., Soong T.W., Sutton K., Slaymaker S., Mathews E., Monteil A., Zamponi G.W., Nargeot J., Snutch T.P. 1999. Splicing of alpha 1A subunit gene generates phenotypic variants of P- and Q-type calcium channels. Nat Neurosci. 5: 407-15.

10. Calin-Jageman I., Yu K., Hall R.A., Mei L., Lee A. 2007. Erbin enhances voltage-dependent facilitation of Ca(v)1.3 Ca2+ channels through relief of an autoinhibitory domain in the Ca(v)1.3 alpha1 subunit. J Neurosci. 6: 1374-85.

11. Castiglioni A.J., Raingo J., Lipscombe D. 2006. Alternative splicing in the C-terminus of CaV2.2 controls expression and gating of N-type calcium channels. J Physiol. 1: 119-34.

12. Catterall W.A. 2000. Structure and regulation of voltage-gated Ca2+ channels. Annu. Rev Cell Dev Biol. 16: 521-55.

13. Catterall W.A., Hulme J.T., Jiang X., Few W.P. 2006. Regulation of sodium and calcium channels by signaling complexes. J Recept Signal Transduct Res 5-6: 577-98.

14. Catterall W.A., Perez-Reyes E., Snutch T.P., Striessnig J. 2005 International Union of Pharmacology. XLVIII. Nomenclature and structure-function

relationships of voltage-gated calcium channels. Pharmacol Rev. 4: 411-25.

15. Cens T., Restituito S., Vallentin A., Charnet P. 1998. Promotion and inhibition of L-type Ca2+ channel facilitation by distinct domains of the subunit. J Biol Chem. 29: 18308-15.

16. Chang C.F., Gutierrez L.M., Mundina-Weilenmann C., Hosey M.M. 1991. Dihydropyridine-sensitive calcium channels from skeletal muscle. II. Functional effects of differential phosphorylation of channel subunits. J Biol Chem. 25: 16395-400.

17. Chemin J., Monteil A., Dubel S., Nargeot J., Lory P., 2001. The alpha1I T-type calcium channel exhibits faster gating properties when overexpressed in neuroblastoma/glioma NG 108-15 cells. Eur. J. Neurosci. 14: 1678-86.

18. Cooper T.A. 2005. Alternative splicing regulation impacts heart development. Cell.120: 1-2

19. De Jongh K.S., Warner C., Colvin A.A., Catterall W.A. 1991. Characterization of the two size forms of the alpha 1 subunit of skeletal muscle L-type calcium channels. Proc Natl Acad Sci USA. 23: 10778-82.

20. De Jongh K.S., Colvin A.A., Wang K.K., Catterall W.A. 1994. Differential proteolysis of the full-length form of the L-type calcium channel alpha 1 subunit by calpain. J Neurochem. 63: 1558–64.

21. De Jongh K.S., Murphy B.J., Colvin A.A., Hell J.W., Takahashi M., Catterall W.A. 1996. Specific phosphorylation of a site in the full-length form of the alpha 1 subunit of the cardiac L-type calcium channel by adenosine 3',5'-cyclic monophosphate-dependent protein kinase. Biochemistry. 32: 10392-402.

22. Diebold R. J., Koch W. J., Ellinor P. T., Wang J. J., Muthuchammy M., Wieczorek D. F., Schwartz A. 1992. Mutually exclusive exon splicing of the cardiac calcium channel α1 subunit gene generates developmentally regulated isoforms in the rat heart. Proc. Natl. Acad. Sci. USA 89: 1497-1501.

23. Dulhunty A.F. 2006. Excitation-contraction coupling from the 1950s into the new millennium. Clin Exp Pharmacol Physiol. 9: 763-72.

24. Erickson M. G., Liang H., Mori M. X., Yue D. T. 2003. FRET two-hybrid mapping reveals function and location of L-type Ca2+ channel CaM preassociation. Neuron 39: 97-107

25. Ertel E.A., Campbell K.P., Harpold M.M., Hofmann F., Mori Y., Perez-Reyes E., Schwartz A., Snutch T.P., Tanabe T., Birnbaumer L., Tsien R.W., Catterall W.A. 2000. Nomenclature of voltage-gated calcium channels. Neuron 25: 533–535.

26. Fearon I.M., Varadi G., Koch S., Isaacsohn I., Ball S.G., Peers C. 2000. Splice variants reveal the region involved in oxygen sensing by recombinant human L-type Ca(2+) channels. Circ Res. 7: 537-9.

27. Flucher B.E., Andrews S.B., Daniels M.P. 1994. Molecular organization of transverse tubule/sarcoplasmic reticulum junctions during development of excitation-contraction coupling in skeletal muscle. Mol. Biol. Cell 5: 1105–1118

28. Flucher B.E., Kasielke N., Gerster U., Neuhuber B., Grabner M. 2000. Insertion of the full-length calcium channel alpha(1S) subunit into triads of skeletal muscle in vitro. FEBS Lett. 1: 93-8.

29. Flucher B.E., Weiss R.G., Grabner M. 2002. Cooperation of two-domain Ca(2+) channel fragments in triad targeting and restoration of excitation- contraction coupling in skeletal muscle. Proc Natl Acad Sci USA. 15: 10167-72.

30. Freise D., Held B., Wissenbach U., Pfeifer A., Trost C., Himmerkus N., Schweig U., Freichel M., Biel M., Hofmann F., Hoth M., Flockerzi V. 2000. Absence of the gamma subunit of the skeletal muscle dihydropyridine receptor increases L-type Ca2+ currents and alters channel inactivation properties. J Biol Chem. 19: 14476-81.

31. Gao T., Cuadra A.E., Ma H., Bunemann M., Gerhardstein B.L., Cheng T., Eick R.T., Hosey M.M. 2001. C-terminal fragments of the alpha 1C (CaV1.2) subunit associate with and regulate L-type calcium channels containing C-terminal-truncated alpha 1C subunits. J Biol Chem. 24: 21089-97.

32. Gomez-Ospina N., Tsuruta F., Barreto-Chang O., Hu L., Dolmetsch R. 2006. The C terminus of the L-type voltage-gated calcium channel Ca(V)1.2 encodes a transcription factor. Cell. 3: 591-606.

33. Goodwin L.O., Leeds N.B., Guzowski D., Hurley I.R., Pergolizzi R.G., Benoff S. 1999. Identification of structural elements of the testis-specific voltage dependent calcium channel that potentially regulate its biophysical properties. Mol Hum Reprod. 4: 311-22.

34. Goren A., Ram O., Amit M., Keren H., Lev-Maor G., Vig I., Pupko T., Ast G. 2006. Comparative analysis identifies exonic splicing regulatory sequences--The complex definition of enhancers and silencers. Molecular Cell 22: 769–81.

35. Gregg R.G., Messing A., Strube C., Beurg M., Moss R., Behan M., Sukhareva M., Haynes S., Powell J.A., Coronado R., Powers P.A. 1996. Absence of the β subunit (cchb1) of the skeletal muscle dihydropyridine receptor alters expression of the α1 subunit and eliminates excitation-contraction coupling. Proc Natl Acad Sci USA. 24: 13961-66.

36. Hell J.W., Westenbroek R.E., Warner C., Ahlijanian M.K., Prystay W., Gilbert M.M., Snutch T.P., Catterall W.A. 1993. Identification and differential subcellular localization of the neuronal class C and class D L type calcium channel alpha 1 subunits. J Cell Biol. 123: 949-62.

37. Hell J.W., Yokoyama C.T., Wong S.T., Warner C., Snutch T.P., CatterallW.A. 1993. Differential phosphorylation of two size forms of the neuronal class C L-type calcium channel α1 subunit. J Biol Chem. 268: 19451-57.

38. Helton T.D., Horne W.A. 2002. Alternative splicing of the beta 4 subunit has alpha1 subunit subtype-specific effects on Ca2+ channel gating. J Neurosci. 5: 1573-82.

39. Hess P. 1990. Calcium channels in vertebrate cells. Annu Rev Neurosci.13: 337-56.

40. Hockerman G.H., Peterson B.Z., Johnson B.D., Catterall W.A. 1997. Molecular determinants of drug binding and action on L-type calcium channels. Annu Rev Pharmacol Toxicol. 37: 361-96.

41. Hulme J.T., Konoki K., Lin T.W., Gritsenko M.A., Camp D.G. II, Bigelow D.J., Catterall W.A. 2005. Sites of proteolytic processing and noncovalent association of the distal C-terminal domain of CaV1.1 channels in skeletal muscle. Proc Natl Acad Sci USA 14: 5274-5279.

42. Hulme J.T., Yarov-Yarovoy V., Lin T.W., Scheuer T., Catterall W.A. 2006. Autoinhibitory control of the CaV1.2 channel by its proteolytically processed distal C-terminal domain. J Physiol. 576(Pt 1): 87-102.

43. International Human Genome Sequencing Consortium. 2004. Finishing the euchromatic sequence of the human genome. Nature 431: 931-45.

44. Ivanina T., Blumenstein Y., Shistik E., Barzilai R., Dascal N. 2000. Modulation of L-type Ca2+ Channels by Gβγ and Calmodulin via Interactions with N and C Termini of α1C. J. Biol. Chem. 275: 39846-54

45. Jurkat-Rott K., Fauler M., Lehmann-Horn F. 2006. Ion channels and ion transporters of the transverse tubular system of skeletal muscle. J Muscle Res Cell Moti. 5-7: 275-90.

46. Jurkat-Rott K., Lehmann-Horn F. 2004. The impact of splice isoforms on voltage-gated calcium channel alpha1 subunits. J Physiol. 3: 609-19.

47. Kanumilli S., Tringham E.W., Payne C.E., Dupere J.R., Venkateswarlu K., Usowicz M.M. 2006. Alternative splicing generates a smaller assortment of CaV2.1 transcripts in cerebellar Purkinje cells than in the cerebellum. Physiol Genomics. 2: 86-96.

48. Kepplinger K.J., Kahr H., Forstner G., Sonnleitner M., Schindler H., Schmidt T., Groschner K., Soldatov N.M., Romanin C. 2000. A sequence in the carboxy-terminus of the alpha(1C) subunit important for targeting, conductance and open probability of L-type Ca(2+) channels. FEBS Lett. 3: 161-9.

49. Kollmar R., Fak J., Montgomery L.G., Hudspeth A.J. 1997. Hair cell-specific splicing of mRNA for the alpha1D subunit of voltage-gated Ca2+ channels in the chicken's cochlea. Proc Natl Acad Sci USA. 26: 14889-93.

50. Kordasiewicz H.B., Thompson R.M., Clark H.B., Gomez C.M. 2006. C-termini of P/Q-type Ca2+ channel alpha1A subunits translocate to nuclei and promote polyglutamine-mediated toxicity. Hum Mol Genet.10: 1587-99.

51. Krovetz H.S., Helton T.D., Crews A.L., Horne W.A. 2000. C-Terminal Alternative Splicing Changes the Gating Properties of a Human Spinal Cord Calcium Channel α1A Subunit. J. Neurosci. 20: 7564-70.

52. Kubodera T., Yokota T., Ohwada K., Ishikawa K., Miura H., Matsuoka T., Mizusawa H. 2003. Proteolytic cleavage and cellular toxicity of the human alpha1A calcium channel in spinocerebellar ataxia type 6. Neurosci Lett. 341: 74-78.

53. Lacinova L., Klugbauer N., Hofmann F. 2000. State- and isoform-dependent interaction of isradipine with the alpha1C L-type calcium channel. Pflugers Arch. 1: 50-60.

54. Lewis B.P., Green R.E., Brenner S.E. 2003. Evidence for the widespread coupling of alternative splicing and nonsense-mediated mRNA decay in humans. Proc Natl Acad Sci USA. 1: 189–92.

55. Li J., Stevens L., Klugbauer N., Wray D. 2004. Roles of molecular regions in determining differences between voltage dependence of activation of CaV3.1 and CaV1.2 calcium channels. J Biol Chem. 26: 26858-67.

56. Lin Z., Haus S., Edgerton J., Lipscombe D. 1997. Identification of functionally distinct isoforms of the N-type Ca2_ channel in rat sympathetic ganglia and brain. Neuron 18: 153–166.

57. Lin Y., McDonough S.I., Lipscombe D. 2004. Alternative splicing in the voltage-sensing region of N-Type CaV2.2 channels modulates channel kinetics. J Neurophysiol. 5: 2820-30.

58. Lipscombe D., Pan J.Q., Gray A.C. 2002. Functional diversity in neuronal voltage-gated calcium channels by alternative splicing of Ca(v)alpha1. Mol Neurobiol. 1: 21-44.

59. Lipscombe D., Helton T., Xu W. 2004. L-type calcium channels: The Low Down. J.Neurophysiology 92: 2633-41.

60. Ma Z., Lou X.J., Horrigan F. 2006.TRole of charged residues in the S1-S4 voltage sensor of BK channels. J Gen Physiol. 3: 309-28.

61. Malouf N.N., McMahon D.K., Hainsworth C.N., Kay B.K. 1992. A two-motif isoform of the major calcium channel subunit in skeletal muscle. Neuron 8: 899–906

62. Marban E., Yamagishi T., Tomaselli G.F. 1998. Structure and function of voltage-gated sodium channels. J Physiol. 508 (Pt 3): 647-57.

63. Margolskee R.F., McHendry-Rinde B., Horn R. 1993. Panning transfected cells for electrophysiological studies. Biotechniques. 5: 906-11.

64. Matlin A.J., Clark F., Smith C.W.J. 2005. Understanding alternative splicing; towards a cellular code. Nature Reviews Mol. Cell. Biol. 6: 386-98.

65. Maximov A., Sudhof T.C., Bezprozvanny I. 1999. Association of neuronal calcium channels with modular adaptor proteins. J Biol Chem 274: 24453–56.

66. McCleskey E.W., Womack M.D., Fieber L.A. 1993. Structural properties of voltage-dependent calcium channels. Int Rev Cytol; 137: 39–54.

67. Melzer W., Herrmann-Frank A., Luttgau H.C. 1995. The role of Ca2+ ions in excitation-contraction coupling of skeletal muscle fibres. Biochim Biophys Acta. 1: 59-116.

68. Melzer W., Andronache Z., Ursu D. 2006. Functional roles of the gamma subunit of the skeletal muscle DHP-receptor. J Muscle Res Cell Motil. 5-7: 307-14.

69. Mori Y., Mikala G., Varadi G., Kobayashi T., Koch S., Wakamori M., Schwartz A. 1996. Molecular pharmacology of voltage-dependent calcium channels. Jpn J Pharmacol. 2: 83-109.

70. Morrill J.A., Cannon S.C. 2000. COOH-terminal truncated alpha(1S) subunits conduct current better than full-length dihydropyridine receptors. J Gen Physiol. 3: 341-8.

71. Mundina-Weilenmann C., Ma J., Rios E., Hosey M.M. 1991. Dihydropyridine-sensitive skeletal muscle Ca channels in polarized planar bilayers. 2. Effects of phosphorylation by cAMP-dependent protein kinase. Biophys J. 4: 902-9.

72. Murbartian J., Arias J.M., Lee J.H., Gomora J.C., Perez-Reyes E. 2002. Alternative splicing of the rat Ca(v)3.3 T-type calcium channel gene produces variants with distinct functional properties. FEBS Lett. 1-3: 272-8.

73. Murbartian J., Arias J.M., Perez-Reyes E. 2004. Functional impact of alternative splicing of human T-type Cav3.3 calcium channels. J Neurophysiol. 6: 3399-407.

74. Nagy E., Maquat L.E. 1998. A rule for termination-codon position within intron-containing genes: when nonsense affects RNA abundance. Trends Biochem Sci. 6: 198-9.

75. Neuhuber B., Gerster U., Döring F., Glossmann H., Tanabe T., Flucher B.E. 1998. Association of calcium channel α1S and β1a subunits is required for the targeting of β1a but not of α1S into skeletal muscle triads. Proc Natl Acad Sci USA. 9: 5015-20.

76. Neves G., Zucker J., Daly M., Chess A. 2004. Stochastic yet biased expression of multiple Dscam splice variants by individual cells. Nat Genet. 3: 240-6.

77. Nilsen T.W. 2003. The spliceosome: the most complex macromolecular machine in the cell? Bioessays. 12: 1147-9.

78. Obermair G.J., Kugler G., Baumgartner S., Tuluc P., Grabner M., Flucher B.E. 2005. The Ca2+ channel alpha2delta-1 subunit determines Ca2+ current kinetics in skeletal muscle but not targeting of alpha1S or excitation-contraction coupling. J Biol Chem. 3: 2229-37.

79. Okagaki R., Izumi H., Okada T., Nagahora H., Nakajo K., Okamura Y. 2001. The maternal transcript for truncated voltage-dependent Ca2+ channels in the ascidian embryo: a potential suppressive role in Ca2+ channel expression. Dev Biol. 2: 258-77.

80. Page K.M., Heblich F., Davies A., Butcher A.J., Leroy J., Bertaso F., Pratt W.S., Dolphin A.C. 2004. Dominant-negative calcium channel suppression by truncated constructs involves a kinase implicated in the unfolded protein response. J Neurosci. 23: 5400-9.

81. Perez-Reyes E., Wei X., Castellano A., Birnbaumer L. 1990. Molecular diversity of L-type calcium channels. Evidence for alternative splicing of the transcripts of three non-allelic genes. J. Biol. Chem. 265:20430-36.

82. Powell J.A., Petherbridge L., Flucher B.E. 1996. Formation of triads without the dihydropyridine receptor alpha subunits in cell lines from dysgenic skeletal muscle. J Cell Biol. 2: 375-87.

83. Ramakrishnan N.A., Green G.E., Pasha R., Drescher M.J., Swanson G.S., Perin P.C., Lakhani R.S., Ahsan S.F., Hatfield J.S., Khan K.M., Drescher D.G. 2002. Voltage-gated Ca2+ channel Ca(V)1.3 subunit expressed in the hair cell epithelium of the sacculus of the trout Oncorhynchus mykiss: cloning and comparison across vertebrate classes. Brain Res Mol Brain Res.1-2: 69-83.

84. Robertson D., Paki B. 2002. Role of L-type Ca2+ channels in transmitter release from mammalian inner hair cells. II. Single-neuron activity. J Neurophysiol. 6: 2734-40.

85. Rousset M., Cens T., Charnet P. 2005. Alone at last! New functions for Ca2+ channel beta subunits? Sci STKE. 275: pe11.

86. Schredelseker J., Di Biase V., Obermair G.J., Felder E.T., Flucher B.E., Franzini-Armstrong C., Grabner M. 2005. The β1a subunit is essential for the assembly of dihydropyridine-receptor arrays in skeletal muscle. Proc Natl Acad Sci 47: 17219-24

87. Scott V. E., Felix R., Arikkath J., Campbell K. P. 1998. Evidence for a 95 kDa short form of the alpha1A subunit associated with the omega-conotoxin MVIIC receptor of the P/Q-type Ca2+ channels. J. Neurosci. 18, 641-647)

88. Seoh S., Sigg D., Papazian D., Bezanilla F. 1996. Voltage-Sensing Residues in the S2 and S4 Segments of the K Channel. Neuron, 16: 1159-67

89. Shen Y., Yu D., Hiel H., Liao P., Yue D.T., Fuchs P.A., Soong T.W. 2006. Alternative splicing of the Ca(v)1.3 channel IQ domain, a molecular switch for Ca2+-dependent inactivation within auditory hair cells. J Neurosci. 42: 10690-9.

90. Soldatov N.M., Bouron A., Reuter H. 1995. Different voltage-dependent inhibition by dihydropyridines of human Ca2+ channel splice variants. J Biol Chem. 18: 10540-3.

91. Soldatov N.M., Zuhlke R.D., Bouron A., Reuter H. 1997.Molecular structures

involved in L-type calcium channel inactivation. Role of the carboxyl-terminal region encoded by exons 40-42 in alpha1C subunit in the kinetics and Ca2+ dependence of inactivation. J Biol Chem. 6: 3560-6.

92. Soong T.W., DeMaria C.D., Alvania R.S., Zweifel L.S., Liang M.C., Mittman S., Agnew W.S., Yue D.T.. 2002. Systematic identification of splice variants in human P/Q-type channel alpha1 (2.1) subunits: implications for current density and Ca2+-dependent inactivation. J Neurosci. 23: 10142-52.

93. Sperelakis N., Shigenobu K. 1972. Changes in membrane properties of chick embryonic hearts during development. J Gen Physiol. 4: 430-53.

94. Stamm S., Zhu J., Nakai K., Stoilov P., Stoss O., Zhang M.Q. 2000. An alternative-exon database and its statistical analysis. DNA Cell Biol. 12: 739-56.

95. Stamm S., Ben-Ari S., Rafalska I., Tang Y., Zhang Z., Toiber D., Thanaraj T.A., Soreq H. 2005. Function of alternative splicing. Gene. 344: 1-20.

96. Stoilov P., Meshorer E., Gencheva M., Glick D., Soreq H., Stamm S. 2002. Defects in pre-mRNA processing as causes of and predisposition to diseases. DNA Cell Biol. 11: 803-18.

97. Takahashi S.X., Mittman S., Colecraft H.M. 2003. Distinctive modulatory effects of five human auxiliary beta2 subunit splice variants on L-type calcium channel gating. Biophys J. 5: 3007-21.

98. Tang Z.Z., Liang M.C., Lu S., Yu D., Yu C.Y., Yue D.T., Soong T.W. 2004. Transcript scanning reveals novel and extensive splice variations in human l-type voltage-gated calcium channel, Cav1.2 alpha1 subunit. J Biol Chem. 43: 44335-43.

99. Tang Z.Z., Hong X., Wang J., Soong T.W. 2007. Signature combinatorial splicing profiles of rat cardiac- and smooth-muscle Ca(v)1.2 channels with distinct biophysical properties. Cell Calcium. 5: 417-28.

100. Westenbroek R.E., Hell J.W., Warner C., Dubel S.J., Snutch T.P., Catterall W.A. 1992. Biochemical properties and subcellular distribution of an N-type calcium channel alpha 1 subunit. Neuron. 9: 1099-115.

101. Yamakage M., Namiki A. 2002. Calcium channels - basic aspects of their structure, function and gene encoding; anesthetic action on the channels - a review. Can J Anaesth. 2: 151-64.

102. Yang L., Liu G., Zakharov S.I., Morrow J.P., Rybin V.O., Steinberg S.F., Marx S.O. 2005. Ser1928 is a common site for Cav1.2 phosphorylation by protein kinase C isoforms. J Biol Chem. 1:207-14.

103. Zuhlke R.D., Bouron A., Soldatov N.M., Reuter H. 1998. Ca2+ channel sensitivity towards the blocker isradipine is affected by alternative splicing of the human alpha1C subunit gene. FEBS Lett. 2: 220-4.

VII. ACKNOWLEDGEMENTS

My sincere thanks to Prof. Frank Lehmann-Horn for giving me opportunity to study in the Department of Applied Physiology, University of Ulm.

I would like to especially thank to my supervisor, PD Dr. Karin Jurkat-Rott for giving me the opportunity to work in her lab and for her support during my Ph.D. research. I would also want to thank her for her enthusiasm for research, beneficial discussions, help and guidance during preparations for the defense.

I would like to thank Prof. Bernhard Flucher from University of Innsbruck for collaboration. My special thanks to Petronel Tuluc and his coworkers from University of Innsbruck for performing immunofluorescence analysis and calcium release measurements.

I owe my warm gratitude to Dr. Simona Ursu and Zoita Andronache for their kindness and help both in work and daily convenience.

Many thanks to former and present lab members of the Department of Applied Physiology and Graduate College 460 for their help, friendship and good working atmosphere.

Finally, I am very grateful to my husband and family. It would be impossible to finish my study without their understanding and support. Dziękuję mojej Rodzinie za niezmienne trwanie przy mnie i za wspieranie mnie w najtrudniejszych chwilach.

VIII: CURRICULUM VITAE

PERSONAL DETAILS

Name:	Natalia Molenda (born Zamiara)
Date of birth:	25.09.1979
Place of birth:	Szczecinek, Poland
Nationality:	polish
Marital status:	married

EDUCATION

30.10.2006 – 27.12.2007	Project management course at Berufsförderungswerk, Geschäftsstelle Ulm
01.01. 2004 – 30.06.2006	Graduate College GRK 460 in Ulm, Germany
01.12.2003 – 30.10.2006	PhD studies at Ulm University, Department of Applied Physiology. This work is part of EU Research Training Network "Excitation-contraction coupling and Ca^{2+} signaling in health and disease" (HPRN-CT-2002-00331)
01.10.1998-29.09.2003	Master degree studies in Biotechnology at Agricultural University of Szczecin, Poland Faculty of Biotechnology and Animal Science
01.09.1994-05.06.1998	High School No.2 Koszalin

STUDENT PRACTICE

04.06.2001-29.06.2001	Technische Universität München, Pflanzenzüchtung und Angewandete Genetik Institut

CONFERENCES AND WORKSHOPS

22 – 25.09.2006	Workshop "Splicing regulatory motifs "Erlangen, Germany
26 – 31.03.2006	Workshop "Emerging Topics in Human Functional Genomics and Proteomics" Antalya, Turkey Oral presentation: "Splicing variants of L-type calcium channel"
18-21. 09. 2005	Annual European Muscle Conference 2005 Hortobagy/Debrecen, Hungary Poster and Abstract: N. Molenda, N. Mao, F. Lehmann-Horn, K. Jurkat-Rott. Splice variants of the CACNA1S calcium channel gene. Journal of Muscle Research and Cell Motility Volume 26, 2005
04-07. 04. 2005	Theoretical course "RNA structure and function" ICGEB Trieste, Italy